Noname manuscript No.
(will be inserted by the editor)

Towards an Efficient Global Multidisciplinary Design Optimization algorithm

S. Dubreuil · N. Bartoli · C. Gogu · T. Lefebvre

Received: date / Accepted: date

Abstract This article proposes a new surrogate based Multidisciplinary Design Optimization algorithm. The main idea is to replace each disciplinary solver involved in a non linear Multidisciplinary Analysis by Gaussian Process surrogate models. Although very natural, this approach creates difficulties as the non linearity of the Multidisciplinary Analysis leads to a non Gaussian model of the objective function. However, in order to follow the path of classical Bayesian optimization such as the Efficient Global Optimization algorithm, a dedicated model of the non Gaussian random objective function is proposed. Then, an expected improvement criterion is proposed to enrich the disciplinary Gaussian processes in an iterative procedure, that we call Efficient Global Multidisciplinary Design Optimization (EGMDO). Such an adaptive approach allows to focus the computational budget on areas of the design space relevant only with respect to the optimization problem. The obtained reduction of the number of solvers evaluations is illustrated on a classical MDO test case and on an engineering test case.

Keywords Multidisciplinary Design Optimization · Gaussian Process · Global optimization ·

1 Introduction

This article addresses the numerical resolution of Multidisciplinary Design Optimization (MDO) problems. MDO deals with the optimization of complex systems involving several disciplinary solvers coupled together in a non linear system of equations called Multidisciplinary Design Analysis (MDA). The basic idea of MDO is to solve the optimization problem of a multidisciplinary system by taking into account the interaction between the disciplines instead of optimizing discipline by discipline sequentially. Since the numerous developments of the second part of 20th century (see. Sobieszczanski-Sobieski and Haftka [30] for a review) a constant struggle has been the use of high fidelity models directly in the optimization, without prohibitive computational costs. Indeed finding an optimal design that satisfies the coupling between disciplines (*i.e.* the equilibrium of the multidisciplinary system) generally needs a large number of disciplinary solver evaluations. To tackle this issue several formulations of the MDO problem have been proposed. Historically, among the first and simplest formulations there are the Multidisciplinary Feasible approach (MDF) and the Individual Discipline Feasible approach (IDF) [6]. MDF consists in solving the MDA by a non intrusive coupling of the disciplinary solvers at each iteration of the optimization algorithm, and thus uncouples the

S. Dubreuil
ONERA/DTIS, Université de Toulouse, Toulouse, France
E-mail: sylvain.dubreuil@onera.fr

N. Bartoli
ONERA/DTIS, Université de Toulouse, Toulouse, France

C. Gogu
Université de Toulouse, CNRS, UPS, INSA, ISAE, Mines Albi, Institut Clément Ader (ICA), 3 rue Caroline Aigle, Toulouse F-31400, France

T. Lefebvre
ONERA/DTIS, Université de Toulouse, Toulouse, France

resolution of the optimization problem and the resolution of the MDA non linear system. It offers the advantage to reach a physically relevant solution at each step of the optimization phase, but leads to an important numerical cost as the MDA has to be solved at each iteration of the optimization process. Contrarily, the IDF approach uncouples the disciplinary solvers but couples the resolution of the optimization problem and the resolution of the MDA *i.e.* the optimization algorithm handling both the design variables and the coupling variables. This formulation is generally quite efficient in terms of the number of disciplinary solver evaluations but can be difficult to set up if the number of variables is important. Accordingly several other formulations have been proposed in the literature in order to solve the MDO problem in an efficient way. A review of some of these approaches can be found in [20]. It should be noted that the majority of these approaches only solve an approximation of the original MDO formulations.

One way to further reduce the cost of MDO resolution is to improve the computation of the gradient of the objective function and thus to take advantage of gradient based optimization algorithm. A large literature is devoted to these type of approaches among which the computation of aeroelastic gradient by the adjoined based method is a representative example (see [19] for example). However, although very efficient, these types of approaches are also very intrusive and designed to accurately converge to a local optimum, which can be detrimental in case of complex objective functions. Concerning this last point it is proposed in [32] to replace the classical gradient based optimizer used in MDO formulations by a surrogate based optimizer. More specifically authors of [32] used the Efficient Global Optimization (EGO) by [14] as optimizer in the MDF, IDF and simultaneous analysis and design (SAND) MDO formulations and compared the results with gradient based and genetic optimization algorithms. An analogue idea is proposed in [29] in which a mixed optimization method based on radial basis function and support vector machine is used to handled mixed discrete-continuous MDO problem.

Another way to reduce the cost of MDO resolution is to replace the costly disciplinary solvers by surrogate models. Paiva et al. [21] for example compared the use of different surrogates (polynomials, kriging, artificial neural networks) to replace the individual discipline models in an MDO analysis. Similarly, in Wang et al. [31], surrogate models are build to replace costly disciplinary analysis. In their approach, the disciplinary surrogate models are build in a non adaptive way by selecting the best surrogate model among radial basis function, Gaussian process, support vector regression, each model with different possible kernel functions according to the concurrent surrogate model selection (COSMOS) based on fixed training samples. The same idea is applied in [5] in which a costly computational fluid dynamic analysis is replaced by a Gaussian process surrogate model and in [33] where kriging surrogate models are used to replace disciplinary models in a battery thermal management system. These non adaptive approaches require very accurate surrogate models of the disciplinary solvers over the whole design space to converge towards the global minimum which can then lead to an important numerical cost during their construction.

The aim of the present paper is to introduce a new adaptive surrogate based MDO approach in which each disciplinary solver is replaced by a disciplinary surrogate model constructed adaptively, such as to be accurate only in areas where the multidisciplinary optimum is likely to be. Such an approach has great potential as it allows to uncouple the MDO problem (as the IDF method) and to focus the computation of the costly disciplinary solvers only on interesting areas with respect to the optimization. It could be noted that the idea of disciplinary Gaussian surrogate models constructed in an adaptive way with respect to a given improvement criterion has been recently proposed in [12] in the context of time dependent reliability analysis of a multidisciplinary system, the numerical procedure to deal with the surrogate model uncertainty propagation and the enrichment criterion being however different from the one proposed in the present article. One can also note that, in the context of disciplinary solvers directly chained (no feedback coupling), the use of disciplinary Gaussian processes has been proposed in [18] and [26] for the adaptive construction of a global surrogate model (in the particular case of direct coupling of Gaussian surrogate models this is nevertheless simplified as analytical expressions of mean and variance of the final quantity of interest can be derived analytically).

The present article proposes first to formalize and to study a MDO strategy in which each disciplinary solver is replaced by a Gaussian process surrogate model. A surrogate enrichment criterion, inspired by the Expected Improvement introduced in the EGO algorithm [14], is then proposed to enrich the disciplinary surrogate model based on the uncertainty they induce in the objective function. However, note that, contrarily to the EGO approach, the objective function is not modeled by a Gaussian process. Indeed the probability distribution of the MDA solution and thus of the objective function are in this case unknowns that result from the uncertainty propagation through the non linear random MDA. Approximation of these probability distributions is one of the other main contributions of this paper. A numerical procedure is proposed to compute the probability distribution of the random MDA output and thus to efficiently sample the random objective function. The idea is then to enrich the disciplinary surrogate model in order to

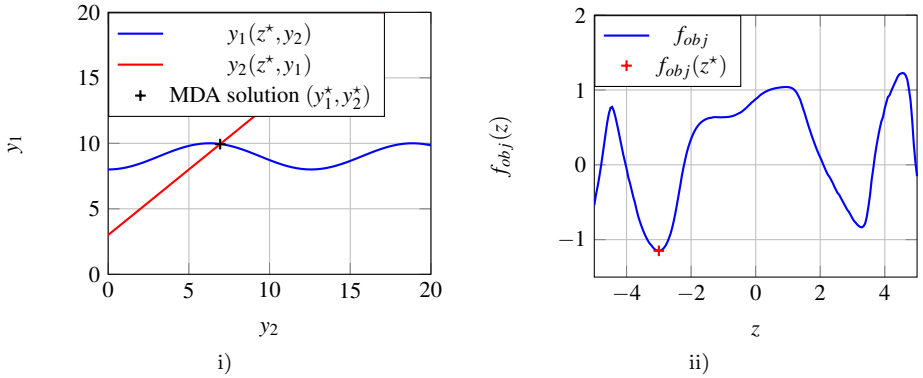

Fig. 1 1-D toy problem. i) Disciplinary solvers and MDA solution at $z^\star$. ii) Objective function and its global minimum.

reduce the uncertainty of the minimum value and associated position. To this purpose an original two-step uncertainty reduction is proposed. It should be noted that this new development aims at extending and improving our previous work on this subject [10].

The rest of this paper is organized as following. First, a 1-D toy problem is introduced in Section 2. This example will help the reader for a better understanding by graphically illustrating the various steps of the proposed method. In Section 3 the proposed algorithm is presented and illustrated on the toy problem. Section 3.2 introduces the way the modeling uncertainties associated with Gaussian process surrogate models is handled. We then derive the random objective function formulation (Section 3.3) and finally present the adaptive disciplinary surrogate enrichment strategy (Section 3.4). The algorithm is summarized in Section 3.5. Section 4 presents an application of the algorithm, quantifying the benefits in terms of computational cost. Concluding remarks are provided in Section 5.

2 Illustrative problem

In order to illustrate the various steps of the proposed approach, the following simple unconstrained MDO problem is introduced and denoted as 1-D toy problem. This problem counts a single scalar design variable $z \in \mathcal{Z} = [-5, 5]$, two scalar coupling variables $y_1 \in \mathbb{R}$ and $y_2 \in \mathbb{R}$ and it is defined by

$$\min_{z \in \mathcal{Z}} f_{obj}(z, y_1^\star, y_2^\star) = \cos\left(\frac{y_1^\star + \exp(-y_2^\star)}{\pi}\right) + \frac{z}{20} \tag{1}$$

where $y_1^\star$ and $y_2^\star$ are solution of the following non linear system of equations, denoted as MDA

$$\begin{cases} y_1(z, y_2) = f_1(z, y_2) = z^2 - \cos\left(\frac{y_2}{2}\right) \\ y_2(z, y_1) = f_2(z, y_1) = z + y_1 \end{cases} \tag{2}$$

The minimum point of this MDO problem is reached for $z^\star \approx -3.0$ leading to $f_{obj}(z^\star) \approx -1.15$. Figure 1 i) presents the coupling between the two disciplines at $z^\star$ *i.e.* $y_1(z^\star, y_2)$ and $y_2(z^\star, y_1)$, the solution of the MDA is characterized by the black cross. Figure 1 ii) presents the objective function as a function of z and the red cross materializes the position of the global minimum.

Next section will proposed a surrogated based approach to solve this MDO problem.

3 Efficient Global Multidisciplinary Optimization

3.1 Introduction

Purpose of the method developed in this article is to solve unconstrained MDO problems of the form, find $z^\star \in \mathcal{Z}$ such as

$$z^\star = \arg\min_{z \in \mathcal{Z}} f_{obj}(z, y^\star_{c^{(obj)}}(z)) \tag{3}$$

where f_{obj} is the objective function to minimize which depends on the design variables z and on some (possibly all) of the converged coupling variables denoted by $y^\star_{c^{(obj)}}(z)$. The design variables z belong to a

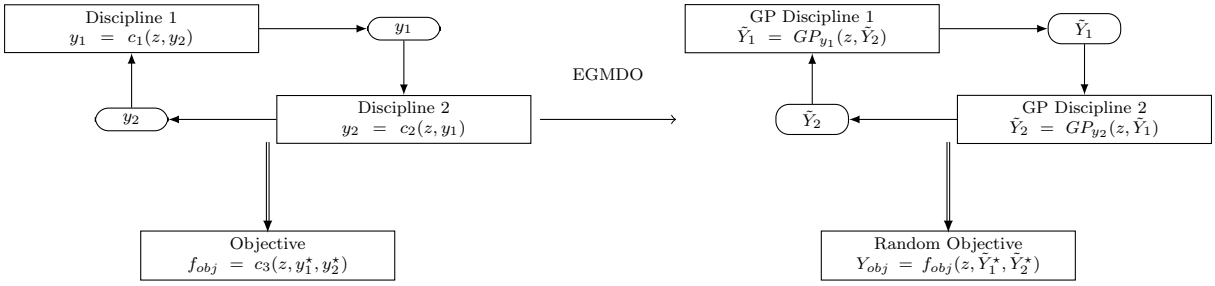

Fig. 2 Illustration of the proposed MDO problem involving two coupled disciplines and an objective function (1-D toy problem). On the left, the disciplines are given by some costly black-boxes. On the right, the disciplines have been replaced by some surrogate models (Gaussian Processes denoted by GP).

design space $\mathcal{Z} \subset \mathbb{R}^n$. The converged coupling variables are denoted by $y^\star(z) = \{y_i^\star(z), i = 1, \cdots, n_d\}$ and $c^{(obj)}$ is a set of indexes used to identify the coupling variables involved in the computation of the objective function. We wrote $y^\star(z)$ the solution of the non linear system of n_d equations, called MDA,

$$y_i = f_i(z, y_{c^{(i)}}),\ i = 1, \cdots, n_d \quad \forall z \in \mathcal{Z} \tag{4}$$

where $y_{c^{(i)}}$ is the vector of the coupling variables for the discipline i and n_d is the number of disciplines. The set of indexes denoted by $c^{(i)}$ identifies the coupling variables *i.e.* $\#(c^{(i)}) \leq (n_d - 1)$ and $i \notin c^{(i)}$. Finally, f_i is the solver of discipline i. Let us note that, with the previously introduced notations, disciplines i and j are said to have a feedback loop if $i \in c^{(j)}$ and $j \in c^{(i)}$. In the following, it is assumed that Eq. (4) contains at least one feedback coupling. It is also assumed that Eq. (4) has a unique solution for any point of the design space.

The starting point of the proposed MDO formulation is to replace all the disciplinary solvers by disciplinary surrogate models and more precisely by Gaussian process surrogate models denoted by GP in the following. In practice the GP that is used to approximate the disciplinary solver f_i is build from a Design of Experiments (denoted by DoE_{f_i}) sampled over the space $\mathcal{Z} \times C^{(i)}$ where $C^{(i)}$ denoted the space of the coupling variables $y_{c^{(i)}}$ for the discipline i. The idea of GP approximation is then to condition a prior GP on DoE_{f_i} and to estimate the parameters of this GP (by maximum likelihood in this work). Readers interested in the construction of GP are referred to [24] for a complete description. In the following random quantities will be denoted by upper case letters. Consequently the disciplinary solver f_i is replaced by,

$$\tilde{Y}_i(z, y_{c^{(i)}}) = \mu_{f_i}(z, y_{c^{(i)}}) + \epsilon_i(z, y_{c^{(i)}}) \tag{5}$$

where $\mu_{f_i}(z, y_{c^{(i)}})$ is the mean function of the GP and $\epsilon_i(z, y_{c^{(i)}})$ is a zero mean GP whose covariance function is the one of the prior GP conditioned on DoE_{f_i}. Thus for a given couple $(z^{(0)}, y_{c^{(i)}}^{(0)}) \in \mathbb{R}^n \times C^{(i)}$, that does not belong to DoE_{f_i} the obtained approximation reads,

$$\tilde{Y}_i(z^{(0)}, y_{c^{(i)}}^{(0)}) = \mu_{f_i}(z^{(0)}, y_{c^{(i)}}^{(0)}) + \sigma_{f_i}(z^{(0)}, y_{c^{(i)}}^{(0)})\xi_i \tag{6}$$

where $\mu_{f_i}(z^{(0)}, y_{c^{(i)}}^{(0)})$ is the mean value, $\sigma_{f_i}(z^{(0)}, y_{c^{(i)}}^{(0)})$ is the standard deviation and ξ_i is a standard Gaussian random variable. It should be noted that the expressions of ϵ_i, μ_{f_i} and σ_{f_i} are fully specified by the kind of Gaussian process approximation used. For conciseness we choose here to not detail the theory of Gaussian process interpolation and refer the reader to [24] instead. In the following, Gaussian process with constant mean and squared exponential covariance function is used.

This strategy is illustrated by Fig. 2 on the 1-D toy example introduced in Section 2.

3.2 Propagation of modeling uncertainty in MDA

The disciplinary GP given by Eq. (6) is now introduced in the MDA (see Eq. (4)) leading to the following random non linear system of n_d equations,

$$\tilde{Y}_i(z, \tilde{Y}_{c^{(i)}}) = \mu_{f_i}(z, \tilde{Y}_{c^{(i)}}) + \epsilon_i(z, \tilde{Y}_{c^{(i)}}),\ i = 1, \cdots, n_d \quad \forall z \in \mathcal{Z} \tag{7}$$

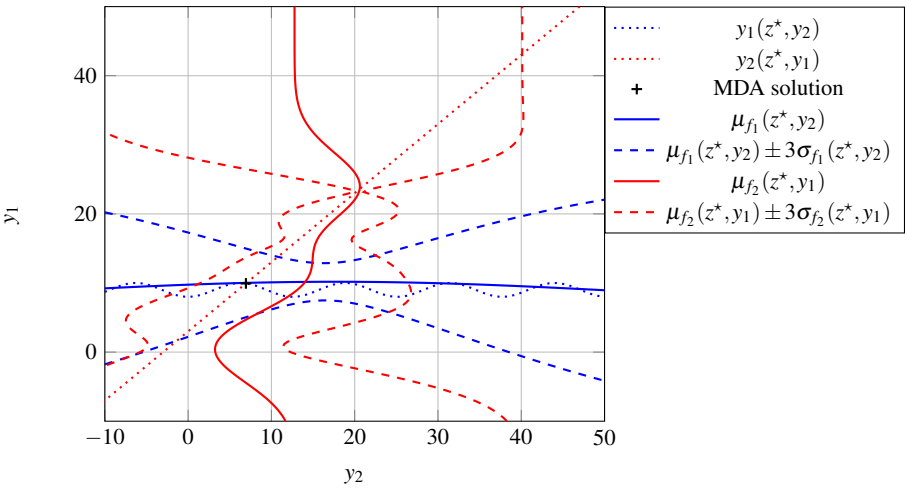

Fig. 3 1-D toy problem. Mean values (solid lines) and 99% confidence intervals (dashed lines) of the two disciplinary GPs at $z^\star$. Actual disciplinary solvers (dotted lines) and MDA solution.

where $\tilde{Y}_{c^{(i)}}$ stands for the random vector of coupling variables affecting the discipline i. We define the solution of this random non linear system of equations as the joined probability distribution of the random vector of the converged coupling variables $\tilde{Y}^\star(z) = \left\{\tilde{Y}_i^\star(z),\ i = 1, \cdots, n_d\right\}$ such as,

$$\tilde{Y}_i^\star(z, \tilde{Y}_{c^{(i)}}^\star(z)) = \mu_{f_i}(z, \tilde{Y}_{c^{(i)}}^\star(z)) + \epsilon_i(z, \tilde{Y}_{c^{(i)}}^\star(z)),\ i = 1, \cdots, n_d \quad \forall z \in \mathcal{Z} \tag{8}$$

Let us underline here that the joined probability density function of $\tilde{Y}^\star(z)$ is not Gaussian as the MDA is a non linear system. Samples of $\tilde{Y}^\star(z)$ can be obtained by drawing various realizations of the GP surrogate models and solving the MDA for each draw. In order to illustrate the solution of such random non linear system of equations the proposed strategy is applied to the 1-D toy example introduced in Section 2 for which $\mathcal{Z} = [-5.0, 5.0]$, $C^{(1)} = [0, 25]$ and $C^{(2)} = [0, 25]$. Disciplinary GPs are constructed with DoE_{f_1} composed of 5 points sampled over $\mathcal{Z} \times C^{(1)}$ and DoE_{f_2} composed of 4 points sampled over $\mathcal{Z} \times C^{(2)}$. Figure 3 presents the two disciplinary GPs with their mean value and their 99% confidence intervals ($\mu \pm 3\sigma$) at $z^\star$. One can note that the actual MDA solution (black cross) is far from the solution obtained with the mean values of the GPs which shows that a direct use of the mean values of the disciplinary GPs (intersection of the blue and the red solid lines associated to $\mu_{f_1}(z^\star, y2)$ and $\mu_{f_2}(z^\star, y1)$) would lead in that case to a large error. However it is also notable that the actual solution of the MDA belongs to the intersection domain of the 99% confidence intervals of the disciplinary GPs which motivates the uncertainty propagation strategy. With respect to this approach Fig. 4 presents three realizations of each disciplinary GP and three associated realizations of the random MDA solution $\tilde{Y}^\star(z^\star) = \left\{\tilde{Y}_1^\star(z^\star), \tilde{Y}_2^\star(z^\star)\right\}$ (black crosses).

Remark:
It should be noted that in this work we are only interested in the variation of the solution set of Eq. (7) which justifies the modeling of the solution by the random vector $\tilde{Y}_i^\star(z)$. In particular we are not interested in the number of solutions for a given random realization, this number being also random. This point is beyond the scope of this article and unnecessary for the purpose of our study. However readers interested in such developments are referred, for example, to [2].

Solving the random non linear system of equations given by Eq. (7) is not straightforward. A direct approach would consist in approximating the random fields ϵ_i by some discretization (either spatially or spectrally) and then to solve the obtained random non linear system of equations parametrized by a finite number of random variables. This number depends of the correlation length of ϵ_i and depending on its value can induce an expensive computational time. This approach has been studied in [8] using Karhunen-Loève decomposition and can lead to an important numerical cost if the number of random variables required to get an accurate approximation of the random fields is important.

Here a more cost-efficient approach is proposed. In order to estimate the probability distribution of $\tilde{Y}^\star(z)$ the idea developed in this section is to solve a simpler system of equations whose solution approximates the distribution of the one of Eq. (7). Indeed, the objective of this uncertainty propagation step is to model the variation of the MDA solutions due to the introduction of disciplinary GP. This variation domain is illustrated on Fig. 3 and Fig. 4 by the intersection of the two confidence intervals (dotted lines). Hence,

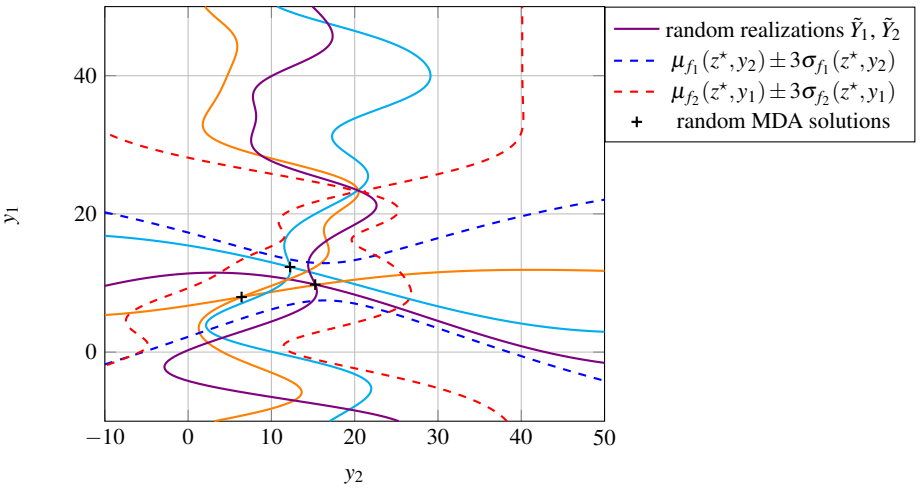

Fig. 4 1-D toy problem. Three random realizations of the disciplinary GPs and corresponding solutions of the random MDA.

one can note that the variation of the MDA solution is driven by the variances of the disciplinary GP. As a consequence we propose to use simplified GP models for the uncertainty propagation task by considering perfectly dependent disciplinary GP whose expression is given by,

$$\tilde{Y}_i'(z) = \mu_{f_i}(z, y_{c^{(i)}}) + \sigma_i(z, y_{c^{(i)}})\xi_i$$

where the variance is computed regarding Eq. (7) by $\forall\ z, y_{c^{(i)}} \in \mathcal{Z} \times \mathbb{R}^{\#c^{(i)}}$, $\sigma_i(z, y_{c^{(i)}})\xi_i = \epsilon_i(z, y_{c^{(i)}})$, with ξ_i a standard Gaussian random variable.

Thus, we propose to solve the system,

$$\tilde{Y}_i'^\star(z, \tilde{Y}_{c^{(i)}}'^\star) = \mu_{f_i}(z, \tilde{Y}_{c^{(i)}}'^\star) + \sigma_i(z, \tilde{Y}_{c^{(i)}}'^\star)\xi_i,\ i = 1, \cdots, n_d \tag{9}$$

whose solution is denoted by the random vector $\tilde{Y}'^\star(z) = \left\{\tilde{Y}_1'^\star(z), \cdots, \tilde{Y}_{n_d}'^\star(z)\right\}$. As the variances of the simplified disciplinary GP involved in Eq. (9) and the one of the disciplinary GP involved in Eq. (7) are equal, we assume that the probability distribution of $\tilde{Y}'^\star(z)$ is a correct approximation of the one of $\tilde{Y}^\star(z)$. It should be noted that the accuracy of this approximation has been numerically checked in [8]. Moreover, from a numerical point of view, Eq. (9) is much more simple to solve than Eq. (7) as it only involves n_d independent standard Gaussian random variables denoted by the vector $\Xi = \{\xi_i,\ i = 1, \cdots, n_d\}$ in the following.

Random MDA has been previously studied and several approaches have been proposed to approximate solution of such a system (see for example [1], [25], [13], [8]). In the following, as the solvers involved in the random MDA are simplified GP, a direct Monte Carlo (MC) method is used. MC simulation consists in solving Eq. (9) for a given realization $\Xi^{(j)}$ of Ξ, for $j = 1, \cdots, n_{MC}$. It should be noted that, for a given realization $\Xi^{(j)}$, any non linear solver can be used to solve these deterministic systems of equations and in the following the non linear Jacobi method is retained. Moreover it should also be noted that these systems of equations can only be solved *pointwise* in the design space *i.e.* for a fixed value $z^{(0)}$ of z. Figure 5 presents the solution of the random MDA for the point $z^\star$ of the 1-D toy example.

The main focus of the next part is to evaluate the influence of the GP surrogate modeling uncertainty of the coupling variables on the objective function.

3.3 Random objective function

First of all let us recall that this paper is interested in MDO problems of the form, find $z^\star \in \mathcal{Z}$ such as

$$z^\star = \arg\min_{z \in \mathcal{Z}} f_{obj}(z, y^\star_{c^{(obj)}}(z)). \tag{10}$$

The previous section has shown that using disciplinary GPs in the MDA leads to random coupling variables denoted by $\tilde{Y}^\star(z) = \left\{\tilde{Y}_i^\star(z),\ i = 1, \cdots, n_d\right\}$. As a consequence, the objective function of the

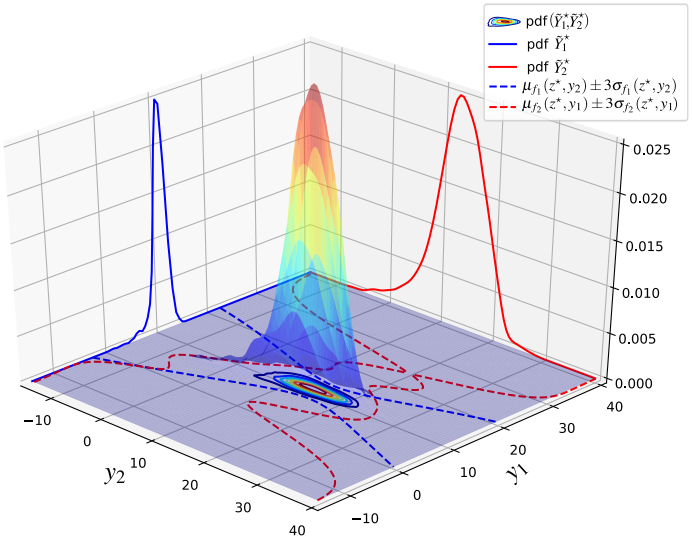

Fig. 5 1-D toy problem. Probability density function of the random MDA solution $(\tilde{Y}_1^\star, \tilde{Y}_2^\star)$ (approximation obtained by MC simulation with and Gaussian kernel smoothing for the illustration).

MDO problem (which is a function of the coupling variables) is also modeled as a random variable or more precisely as a random field over the design space $\mathcal{Z}$,

$$Y_{obj}(z, \tilde{Y}^\star_{c^{(obj)}}(z)) = f_{obj}(z, \tilde{Y}^\star_{c^{(obj)}}(z)),\ \forall z \in \mathcal{Z} \tag{11}$$

The proposed method to characterize this random variable is based on an approximation of $Y_{obj}(z, \tilde{Y}^\star_{c^{(obj)}}(z))$ by polynomial chaos expansion (PCE) [11]. PCE approximation consists in the following decomposition,

$$\hat{Y}_{obj}(z, \Xi) = \sum_{j=1}^{P} a_j^{(obj)}(z) H_j(\Xi) \quad \forall z \in \mathcal{Z} \tag{12}$$

where $H_j,\ j = 1, \cdots, P$ are the n_d-variate Hermite polynomials, P is the number of selected polynomial terms and $a_j^{(obj)}(z),\ j = 1, \cdots, P$ are the coefficients of the expansion to be determined. The retained truncation strategy consists in keeping all the polynomials with a degree less or equal to d, thus $P = \frac{(n_d+d)!}{n_d!d!}$. Computation of these coefficients can be obtained by various approaches. In the following the regression approach introduced in [4] is retained. It should be noted that this method is easy to set up in the context of the study as a large number of samples of $Y_{obj}(z, \tilde{Y}^\star_{c^{(obj)}}(z))$ can be obtained at a very low numerical cost from the MC solution of the random MDA described in Section 3.2. The number of MC simulations will be chosen accordingly to the number P of coefficients to compute. Figure 6 presents the results of PCE approximation of $Y_{obj}(z^\star, \tilde{Y}^\star_{c^{(obj)}}(z^\star))$ compared with the associated MC approximation with $d = 3$ on the 1-D toy example.

It is notable on this 1-D toy example that the distribution of $Y_{obj}(z^\star, \tilde{Y}^\star_{c^{(obj)}}(z^\star))$ is clearly not Gaussian and that a *low degree* PCE $d = 3$ leads to a fair approximation. The PCE approximation allows to compute an approximation of $Y_{obj}(z^\star, \tilde{Y}^\star_{c^{(obj)}}(z^\star)), \forall z \in \mathcal{Z}$ but coefficients $a_j^{(obj)}(z),\ j = 1, \cdots, P$ need to be computed *pointwise i.e.* for a fixed value of z. In the following an original continuous approximation of this random field proposed in [9] that will be further used to explore the design space is introduced.

From now on it is assumed that the uncertainty quantification by PCE has been performed on a DoE denoted by $\text{DoE}_{UQ} = \left\{z^{(i)},\ i = 1, \cdots, n_{UQ}\right\}$. The obtained PCE formed the following random vector

$$\hat{\mathbf{Y}}_{obj}(\Xi) = \left\{\hat{Y}_{obj}(z^{(i)}, \Xi),\ i = 1, \cdots, n_{UQ}\right\}$$

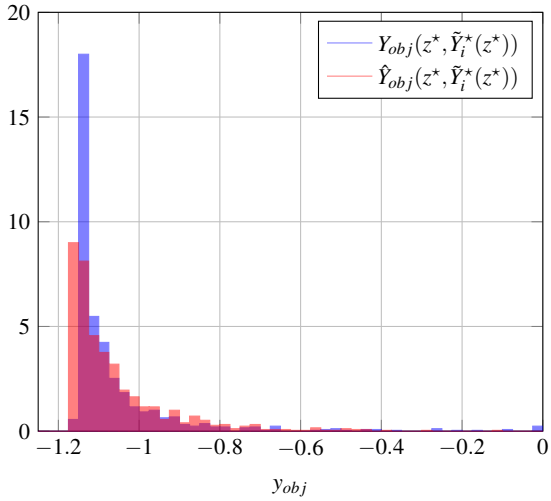

Fig. 6 1-D toy problem. Approximation of the random objective function by PCE of order 3, denoted by $\hat{Y}_{obj}(z^\star, \tilde{Y}^\star_{c^{(obj)}}(z^\star))$, compared with the reference MC result, denoted by $Y_{obj}(z^\star, \tilde{Y}^\star_{c^{(obj)}}(z^\star))$.

The random vector $\hat{\mathbf{Y}}_{obj}$ is a discretization of the random field $\hat{Y}_{obj}(z, \Xi)$. As shown in [1] the Karhunen Loève expansion of this random vector can be easily obtained thanks to the coefficients of the polynomial chaos expansions and reads,

$$\hat{\mathbf{Y}}_{obj}(\Xi) = \mu_{\hat{\mathbf{Y}}_{obj}} + \sum_{k=1}^{n_{UQ}} \left(\sum_{j=2}^{P} \mathbf{a}_j^t \hat{\varphi}_k \phi_j(\Xi) \right) \hat{\varphi}_k \tag{13}$$

where $\mathbf{a}_j = \left\{ a_j^{(obj)}(z^{(1)}), \cdots, a_j^{(obj)}(z^{(n_{UQ})}) \right\}$, $j = 2, \cdots, P$, $\mu_{\hat{\mathbf{Y}}_{obj}} = \mathbf{a}_1$ and $\hat{\varphi}_k$ are the n_{UQ} eigenvectors of the covariance matrix $\mathbf{K}_{\hat{\mathbf{Y}}} = \sum_{i=2}^{P} \mathbf{a}_i \mathbf{a}_i^t$. From Eq. (13) it is proposed in [9] to approximate the random field $\hat{Y}_{obj}(z, \Xi)$ by Gaussian process interpolation of the mean value and of the eigenvectors based on the vectors $\mu_{\hat{\mathbf{Y}}_{obj}}$ and $\hat{\varphi}_k$ respectively. This leads to the following representation of the random field,

$$\hat{Y}_{obj}(z, \Xi) \approx \tilde{Y}_{obj}(z, \Xi, \eta) = \tilde{\mu}_{\hat{\mathbf{Y}}_{obj}}(z, \eta_0) + \sum_{k=1}^{n_{UQ}} \left(\sum_{j=2}^{P} \mathbf{a}_i^t \hat{\varphi}_k \phi_j(\Xi) \right) \tilde{\varphi}_k(z, \eta_k), \ \forall z \in \mathcal{Z} \tag{14}$$

where $\tilde{\mu}_{\hat{\mathbf{Y}}_{obj}}(z, \eta_0)$ and $\tilde{\varphi}_k(z, \eta_k)$ are respectively the GP interpolation of the mean vector $\mu_{\hat{\mathbf{Y}}_{obj}}$ and of the eigenvectors $\hat{\varphi}_k$. The term $\eta = [\eta_0, \cdots, \eta_k, \cdots, \eta_{n_{UQ}}]^t$ is a random vector of $n_{UQ} + 1$ independent normal random variables modeling the uncertainty associated with these GP interpolations. At this point, two remarks can be made.

- In practice we observed that the random vector $\hat{\mathbf{Y}}_{obj}(\Xi)$ is generally strongly correlated. Hence the Karhunen Loève expansion, given by Eq. (13), can be accurately approximated by truncating it to the M eigenvectors associated to the M highest eigenvalues of the covariance matrix. In practical applications we often observed $M \ll n_{UQ}$ while M is chosen so that the cumulative sum of the M highest eigenvalues is strictly higher than $1 - 10^{-6}$. This remark is very important in practice as it allows to limit the number of GP interpolations to construct.
- As Gaussian processes have been used twice, two different denominations will be used in the following:
  - to approximate each disciplinary solver f_i (see Eq. (6)) are denoted **disciplinary GP**,
  - to approximate the mean value and the eigenvectors of the Karhunen Loève decomposition (see Eq. (14)) are denoted **KL-GP**.

One can note that the approximation of the random field modeling the objective function (Eq. (14)) depends on two sources of uncertainty. The first one, modeled by the random vector Ξ, is due to the use of disciplinary GP surrogate models in the multidisciplinary analysis. The second one, modeled by the random vector η, is due to the interpolation of the discretization of the random field modelling the random objective function. It is also notable that Eq. (14) can be evaluated analytically for all points of the design space and for all realizations of the random vectors Ξ and η. Thus, it is a valuable tool to rapidly explore the

objective function with respect to the design variables by considering both sources of uncertainty previously introduced. Before moving to the next section, the proposed approximation is illustrated on the 1-D toy example. To this purpose DoE_{UQ} is defined with $n_{UQ} = 4$ points as

$$\text{DoE}_{UQ} = \{-4.3, -2.5, 0.5, 3.7\}$$

Figure 7 presents the KL-GP interpolations of the mean function $\tilde{\mu}_{\hat{\mathbf{Y}}_{obj}}(z, \eta_0)$ (Fig. 7 i)) and the two first eigenvectors $\tilde{\varphi}_k(z, \eta_k)$ (Fig 7 ii) and iii)). These figures allow to visualize the effect of the uncertainty associated to the KL-GP interpolation in the representation of the random field modeling the objective function. Hence these figures only represent the uncertainty linked to the discretization of the objective function random field with respect to the design variables and modeled by the random vector η. The uncertainty due to the use of the two disciplinary surrogate models (modeled by the random vector Ξ) that affect the terms $\mathbf{a}_i^t \hat{\varphi}_k \phi_i(\Xi)$ of Eq. (14) is illustrated by Fig. 8 which presents some random realizations of the proposed random field approximation (Eq. (14)). It should be noted that contrarily to the KL-GP interpolation of the mean function and of the eigenvectors, the random field obtained by combining both sources of uncertainty is no longer Gaussian. Moreover, Fig. 8 presents the actual value of the objective function. One can note that the random field obtained using the disciplinary GP is far from being accurate enough to localize the minimum of the deterministic objective function. On this illustrative example, with only five evaluations of discipline 1 and four evaluations of discipline 2, it already allows to conclude that the minimum of the objective function is probably not localized in the neighborhood of 0.

At this point we would like to make a few comments regarding the way noise may affect the proposed approach. Indeed numerical noise can exist at multiple stages:

- we can have numerical noise in disciplinary simulations that would affect the disciplinary Gaussian processes (GP), which were considered interpolating here. We assume here that the disciplinary simulations are sufficiently converged such that the associated noise is negligible.
- we can have numerical noise in the PCE. This depends on the variance of the estimation of the PCE coefficients (size of the random samples and truncature degree). First, note that in our case, the size of the random samples is large since the MDA is solved using the disciplinary GPs (numerically inexpensive). Second, note also, that even in presence of noise, the PCE is used to construct a KL expansion over the design space. This KL expansion will tend to filter out noise, since we truncate the expansion at order M.
- interpolating GP approximations are again constructed on the mean and eigenvectors of the KL expansion. As explained in the previous point, as only the dominant modes of the KL expansion are kept, we do not expect to have significant noise at this stage. There may however be bias in the approximations if the PCE is poorly converged, thus biasing the KL expansion.

We think that for many problems the noise at these three stages can be kept in check by a careful analysis of the convergences. If appropriate convergence is intractable and one has to settle with non-negligible noise levels, then noisy kriging [22] could be considered and adapted.

Finally note that the construction of the KL-GP interpolation may appear quite complex. Other, simpler approaches (direct interpolation of the PCE coefficients by GPs), have been investigated by the authors in a somewhat different context in [9] and were found to be less efficient numerically, which is why we settled for the approach as it is proposed currently.

Next section further exploits this idea and presents a criterion devoted to find the relevant point of the design space where the accuracy of the random field approximation given by Eq. (14) should be increased, in order to get a surrogate-based optimum more accurate.

3.4 Adaptive strategy, uncertainty reduction

As explained in the introduction the purpose here is to solve a deterministic MDO problem by using disciplinary surrogate models. The previous section has shown how the uncertainties associated to each disciplinary GP can be efficiently propagated to the objective function and how this random objective function can be modelled as a random field over the design space (see Eq. (14)). Objective of this section is to reduce the uncertainty of the random objective function in the areas of the design space where the minimum is likely to be. As in the EGO (Efficient Global Optimization [14]) algorithm, an exploration criterion is proposed; however contrarily to the EGO algorithm (where only the interpolation uncertainty has to be considered), the uncertainty of the random objective function depends on two sources of uncertainty. As a consequence a two-step uncertainty reduction approach is proposed.

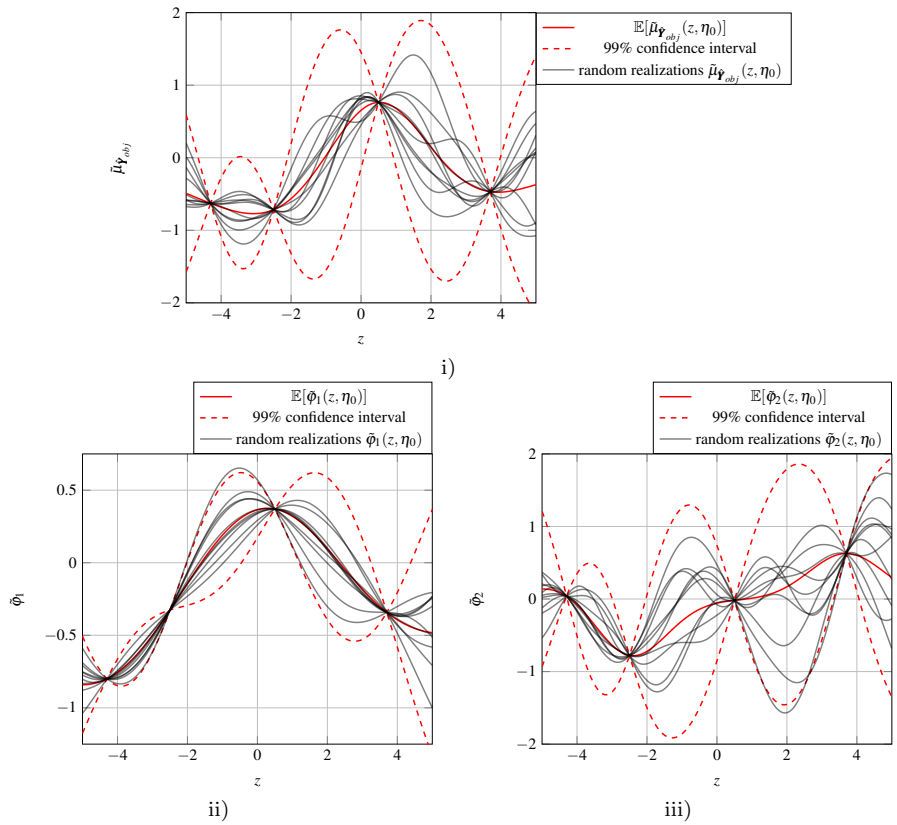

Fig. 7 1-D toy problem. Illustration of the GP interpolation used in Eq. (14). Mean GP approximation (red solid line), 99% confidence interval (dashed red lines), random realizations (black solid lines) i) Mean value of the KL decomposition ii) First eigenvector of the KL decomposition iii) Second eigenvector of the KL decomposition.

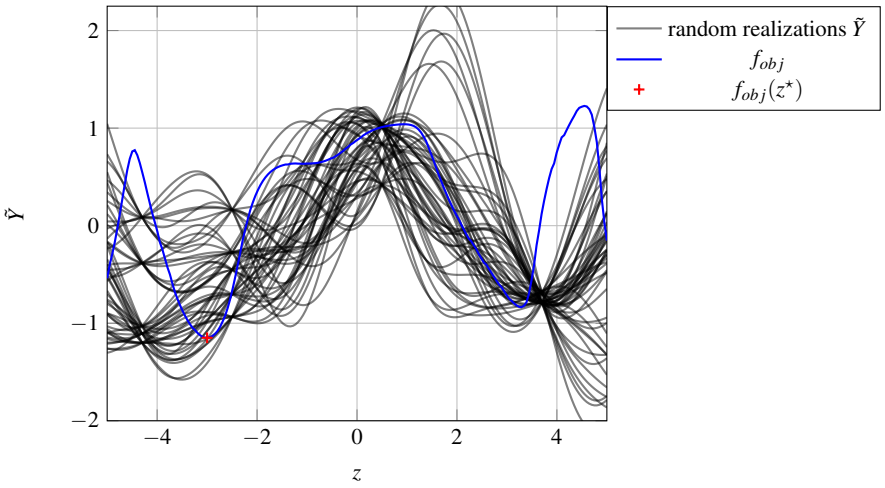

Fig. 8 1-D toy problem. Random realizations (black solid lines) of the approximation proposed by Eq. (14) to model the deterministic objective function (solid blue line) by taking into account the disciplinary GP uncertainty and the interpolation of KL decomposition mean and eigenvectors.

– First a criterion inspired by the Expected Improvement is used in order to determine the point $z^{(new)}$ of the design space where the uncertainty of $\tilde{Y}_{obj}(z, \Xi, \eta)$ should be reduced. It should be noted that this criterion considered both sources of uncertainty, the one due to the disciplinary GP (modeled by Ξ) and the one due to the KL-GP interpolation of the mean and eigenvectors (modeled by η). At this point the random field $\tilde{Y}_{obj}(z, \Xi, \eta)$ is discretized at $z^{(new)}$ *i.e.* uncertainty quantification by PCE is carried out at $z^{(new)}$ leading to $\hat{Y}_{obj}(z^{(new)}, \Xi)$ (eliminating the uncertainty source modeled by η at $z^{(new)}$). This criterion has been developed in [9] and only important steps are recalled in Section 3.4.1.
– The second step focuses on the random vector $\hat{\mathbf{Y}}_{obj}(\Xi)$. The idea of this second step is to reduce the uncertainty only with respect to Ξ by enrichment of the disciplinary GP. This second step is one of the original developments of this article presented in details in Sections 3.4.2 and 3.4.3.

3.4.1 Where to reduce the uncertainty of the random field $\tilde{Y}_{obj}(z, \Xi, \eta)$?

To answer this question, the random variable modeling the minimum value of the continuous random field $\hat{Y}_{obj}(z, \Xi)$, which is the random field obtained by PCE at every point of $\mathcal{Z}$, is defined by,

$$\hat{Y}_{min}^{(obj)}(\Xi) = \min_{z \in \mathcal{Z}} \hat{Y}_{obj}(z, \Xi)$$

and its discretized version,

$$\hat{Y}_{min}^{(obj)}(\Xi) | z \in \mathrm{DoE}_{UQ} = \min_{k=1,\cdots,n_{UQ}} \left\{ \hat{Y}_{obj}(z^{(k)}, \Xi),\ k = 1, \cdots, n_{UQ} \right\} \tag{15}$$

Inspired by the work of [14] on optimization of black-box function by GP, the Expected Improvement with respect to both sources of uncertainties, Ξ and η, is now defined as, $\forall z \in \mathcal{Z}$

$$\mathrm{EI}(z) = \mathbb{E}\left[\left(\hat{Y}_{min}^{(obj)}(\Xi) | z \in \mathrm{DoE}_{UQ} - \tilde{Y}_{obj}(z, \Xi, \eta) \right) \mathbb{1}_{\tilde{Y}_{obj}(z,\Xi,\eta) \leqslant \hat{Y}_{min}^{(obj)}(\Xi) | z \in \mathrm{DoE}_{UQ}} \right] \tag{16}$$

where
$\mathbb{1}_{\tilde{Y}_{obj}(z,\Xi,\eta) \leqslant \hat{Y}_{min}^{(obj)}(\Xi) | z \in \mathrm{DoE}_{UQ}} = 0$ if $\tilde{Y}_{obj}(z, \Xi, \eta) > \hat{Y}_{min}^{(obj)}(\Xi) | z \in \mathrm{DoE}_{UQ}$ and
$\mathbb{1}_{\tilde{Y}_{obj}(z,\Xi,\eta) \leqslant \hat{Y}_{min}^{(obj)}(\Xi) | z \in \mathrm{DoE}_{UQ}} = 1$ if $\tilde{Y}_{obj}(z, \Xi, \eta) \leqslant \hat{Y}_{min}^{(obj)}(\Xi) | z \in \mathrm{DoE}_{UQ}$.
One can note that $\mathrm{EI}(z)$ is positive for $z \notin \mathrm{DoE}_{UQ}$ and that $\mathrm{EI}(z) = 0$ if $z \in \mathrm{DoE}_{UQ}$. The point $z^{(new)}$ where the uncertainty quantification by PCE should be performed is thus solution of the optimization problem,

$$z^{(new)} = \arg \max_{z \in \mathcal{Z}} \left(\mathrm{EI}(z) \right) \tag{17}$$

It can be noticed that at a given point $z^{(0)} \in \mathcal{Z}$, a positive value of the Expected Improvement (as defined by Eq. (16)) could have two reasons:

– Large uncertainty due to the KL-GP interpolation of the design space discretization (modelled by the random vector η) increases the variability of the random variable $\tilde{Y}_{obj}(z^{(0)}, \Xi, \eta)$, thus the random event $\left(\hat{Y}_{min}^{(obj)}(\Xi) | z \in \mathrm{DoE}_{UQ} > \tilde{Y}_{obj}(z^{(0)}, \Xi, \eta) \right)$ may have a non negligible probability. Enrichment in such areas helps the *exploration* of the optimization design space.
– If the uncertainty associated with the KL-GP interpolation of the design space discretization is low (compared to the one due to Ξ), then a large value of $\mathrm{EI}(z)$ means that the random variable $\tilde{Y}_{obj}(z^{(0)}, \Xi, \eta) \approx \hat{Y}_{obj}(z^{(0)}, \Xi)$ contributes significantly to the random variable $\hat{Y}_{min}^{(obj)}(\Xi)$. This means that the uncertainty stemming from the disciplinary GPs approximations is significant at this $z^{(0)}$, and it would be beneficial to reduce it at this point by enrichment of the disciplinary surrogate models.

It should be noted that the EI defined by Eq. (16) is different from the one proposed in [14] in the context of optimization of black-box functions. In particular, as the approximation Eq. (14) is not a Gaussian process, the EI defined by Eq. (16) can not be computed analytically and will be estimated by MC sampling (see [9] for details about estimation and optimization of the EI). Figure 9 presents the EI for the 1-D toy example in the same conditions as Fig. 8.

One can note on Fig. 9 that the EI reaches its maximum in a promising area of the design space $\mathcal{Z}$ ($z^{(new)} \approx -3.5$) and that the other local maxima are located at the bounds of the design space which is coherent with the dispersion of the random field modeling the objective function illustrated on Fig. 8. In addition one can note that the EI value is very low in the neighborhood of $z = 0$ as predicted intuitively in the comments of Fig. 8. However, comparing to the EI defined by [14] one might be surprised by the behavior of the EI depicted by Fig. 9.

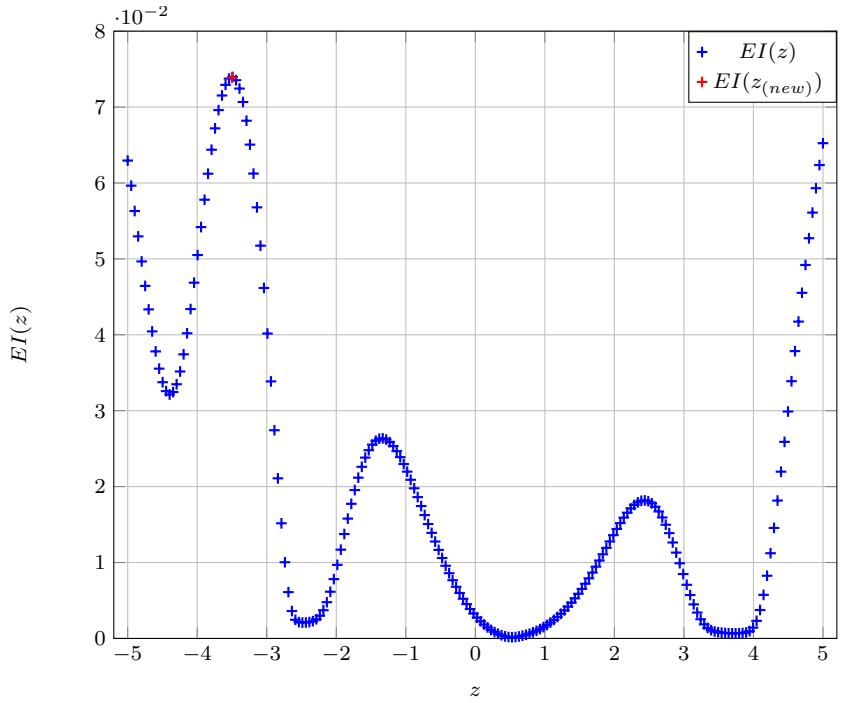

Fig. 9 1-D toy problem. Expected improvement (blue crosses) and its maximum (red cross).

- Firstly, the proposed EI seems not null at points that belongs to DoE_{UQ} (it is especially visible on Fig. 9 at $z = -4.3$), which appears in contradiction with its definition provided by Eq. (16). This can be explained by noting that the DoE_{UQ} points act as singularities and that the variations of EI in their neighborhood can be highly non linear. Indeed, variations of $\tilde{Y}_{obj}(z, \Xi, \eta)$ with respect to the random variable η are expected to be relatively smooth in the neighborhood of the points DoE_{UQ} as, by construction, variation of the Gaussian process only depends on the distance between the current point z and the points of DoE_{UQ}. However the variations of $\tilde{Y}_{obj}(z, \Xi, \eta)$ with respect to the random variable Ξ are arbitrary and lead to the strong non linearities observed around the points of DoE_{UQ}.
- Secondly, the value of the EI depicted by Fig. 9 is relatively low at the optimum of the deterministic problem ($z^\star = -3$). Eventually, if this point belongs to DoE_{UQ}, the EI would be null. However it is important to keep in mind that the purpose of the proposed expected improvement is to find areas of the design space where the random variables $\tilde{Y}_{obj}(z^{(0)}, \Xi, \eta) \approx \hat{Y}_{obj}(z^{(0)}, \Xi)$ contributes significantly to the random variable $\hat{Y}_{min}^{(obj)}(\Xi)$.

The question of reducing the uncertainty of $\hat{Y}_{min}^{(obj)}(\Xi)$ by improving the disciplinary surrogate models will be now studied.

3.4.2 Uncertainty reduction by improvement of the disciplinary GP

Previous section proposed a criterion that allows to identify a point $z^{(new)} \in \mathcal{Z}$ where the uncertainty quantification by PCE needs to be performed in order to improve our knowledge on the random variable modeling the minimum value of the random field $\tilde{Y}_{obj}$. As a consequence this point is added to DoE_{UQ} and the PCE approximation $\hat{Y}_{obj}(z^{(new)}, \Xi)$ is computed and added to the random vector $\hat{\mathbf{Y}}_{obj}(\Xi) = \left\{\hat{Y}_{obj}(z^{(1)}, \Xi), \cdots, \hat{Y}_{obj}(z^{(n_{UQ}-1)}, \Xi), \hat{Y}_{obj}(z^{(new)}, \Xi)\right\}$. Then, thanks to these PCE approximations, it is straightforward to estimate the probability mass function of $\hat{Y}_{min}^{(obj)}(\Xi)|z \in \mathrm{DoE}_{UQ}$ defined by Eq. (15) which is a discrete random variable. Indeed, let us denote by $P_{min}(z^{(i)})$ the probability that $z^{(i)}$ to be the minimum of $\hat{\mathbf{Y}}_{obj}(\Xi)$, its expression reads, $\forall\, i \in [1, \cdots, n_{UQ}]$

$$\begin{aligned} P_{min}(z^{(i)}) &= \mathbb{P}\left(\min \hat{\mathbf{Y}}_{obj}(\Xi) = \hat{Y}_{obj}(z^{(i)}, \Xi)\right) \\ &\approx \tfrac{1}{n_{MC}} \textstyle\sum_{k=1}^{n_{MC}} \mathbb{1}_{\min \hat{\mathbf{Y}}_{obj}(\Xi^{(k)}) = \hat{Y}_{obj}(z^{(i)}, \Xi^{(k)})} \end{aligned} \tag{18}$$

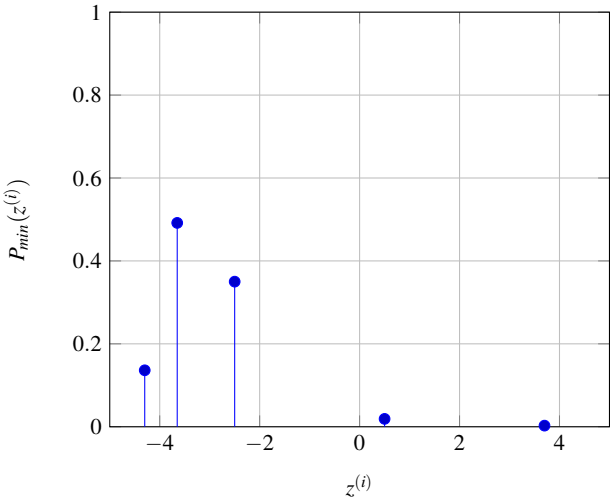

Fig. 10 1-D toy problem. Probability mass function of $\hat{Y}_{min}^{(obj)}(\Xi)|z \in \text{DoE}_{UQ}$ after adding the point $z^{(new)} = -3.5$ to the initial DoE_{UQ}.

It should be noted that the cost of this MC estimation is negligible as it only involves PCE evaluations. From a practical point of view, n_{MC} realizations associated to a value of Ξ are computed, $\hat{Y}_{obj}(z^{(i)})$ is then evaluated for each value of $z^{(i)} \in \text{DoE}_{UQ}$ and the minimum is selected in this set of points. Figure 10 presents the probability mass function of $\hat{Y}_{min}^{(obj)}(\Xi)|z \in \text{DoE}_{UQ}$ on the 1-D toy example.

On this figure one can note that the point added by the EI criterion $z^{(new)} \approx -3.5$ is the one with highest probability of being the minimum of $\hat{Y}_{obj}(z)|z \in \text{DoE}_{UQ}$. This probability density mass function reveals the points where the minimum of the deterministic function might be located. As our objective is to localize this minimum with a high probability, we would like this probability mass function to count a single point $z^\star$ with a significant $P_{min}(z^\star)$ value and more important such that the coefficient of variation of $\hat{Y}(z^\star)$ is low *i.e* the random variable $\hat{Y}(z^\star)$ follows a Dirac probability distribution. To do so, the following algorithm is proposed (see Algo. 1). In Algo. 1 we define the set $Z_{can} = \left\{ z^{(i)}, P_{min}(z^{(i)}) \geq \frac{1}{n_{UQ}},\ i = 1, \cdots, n_{UQ} \right\}$

initialization: Compute PCE approximations, $\hat{Y}_{obj}(z^{(i)}, \Xi), \forall z^{(i)} \in \text{DoE}_{UQ}$
Compute $P_{min}(z^{(i)}),\ \forall z^{(i)} \in \text{DoE}_{UQ}$
while $\exists\ z^{(i)} \in \text{DoE}_{UQ}$ *such that* $P_{min}(z^{(i)}) \geq \frac{1}{n_{UQ}}$ *and* $cv(\hat{Y}_{obj}(z^{(i)})) \geq \epsilon_{cv}$ **do**
  Create the set $Z_{can} = \left\{ z^{(i)}, P_{min}(z^{(i)}) \geq \frac{1}{n_{UQ}},\ i = 1, \cdots, n_{UQ} \right\}$
  Sort Z_{can} in decreasing order with respect to $P_{min}(z^{(i)})$
  Set $k = 0$, $convergence = False$
  while $k < card(Z_{can})$ *and* $pts\_added == False$ **do**
    if $cv(\hat{Y}_{obj}(Z_{can}[k])) \leq \epsilon_{cv}$ **then**
      $k = k + 1$
    else
      Add $Z_{can}[k]$ to the disciplinary GPs (see next section)
      Update the disciplinary GPs
      Compute PCE approximations, $\hat{Y}_{obj}(z^{(i)}, \Xi), \forall z^{(i)} \in \text{DoE}_{UQ}$
      Compute $P_{min}(z^{(i)}),\ \forall z^{(i)} \in \text{DoE}_{UQ}$
      $pts\_added = True$
    end
  end
end

Algorithm 1: Proposed algorithm to reduce the uncertainty on the minimum position of the discrete problem, $\hat{Y}_{obj}(z)|z \in \text{DoE}_{UQ}$

and $cv(\hat{Y}_{obj}(Z_{can}[k])) = \frac{\sqrt{\mathbb{V}ar[\hat{Y}_{obj}(Z_{can}[k])]}}{\mathbb{E}[\hat{Y}_{obj}(Z_{can}[k])]}$ stands for the coefficient of variation of $\hat{Y}_{obj}(Z_{can}[k])$ and ϵ_{cv} is a parameter that controls the maximum value of the coefficients of variation of the interesting points *i.e.*

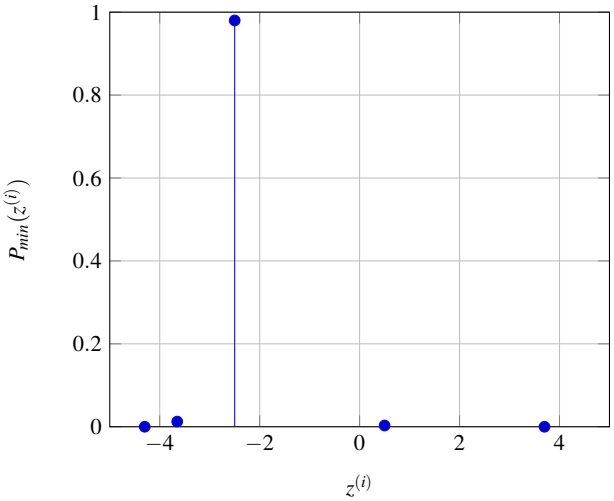

Fig. 11 1-D toy problem. Probability mass function of $\hat{Y}_{min}^{(obj)}(\Xi)|z \in \text{DoE}_{UQ}$. Uncertainty reduction after 5 iterations of Algo. 1 (comparison with the initial probability mass function Fig. 10).

the ones such that $P_{min}(z^{(i)}) \geq \frac{1}{n_{UQ}}$. Note that in the particular case where $\mathbb{E}[\hat{Y}_{obj}(Z_{can}[k])] = 0$, then the coefficient of variation $cv(\hat{Y}_{obj}(Z_{can}[k]))$ is not defined and it is replaced by the direct use of the standard deviation $\sqrt{\mathbb{V}ar[\hat{Y}_{obj}(Z_{can}[k])]}$.

The heuristic proposed in Algo. 1 tends to reduce the uncertainty with respect to the Ξ random variable until the random variable modeling the minimum position of the discrete problem *i.e.* $\hat{Y}_{min}^{(obj)}(\Xi)|z \in \text{DoE}_{UQ}$, reaches a Dirac distribution. It should be noted that the proposed approach is controlled by a single parameter ϵ_{cv}. In practice this parameter is set to $\epsilon_{cv} = 0.01$. Figure 11 presents the probability mass function of $\hat{Y}_{min}^{(obj)}(\Xi)|z \in \text{DoE}_{UQ}$ on the 1-D toy example after convergence of the Algo. 1.

Figure 11 illustrates the uncertainty reduction on the position of the minimum of the discrete problem. Indeed, one can note that $\hat{Y}_{min}^{(obj)}(\Xi)|z \in \text{DoE}_{UQ}$ is almost a Dirac random variable located at $z = -2.5$. In this example, Algo. 1 converges after 5 iterations, next section details how the disciplinary GPs are enriched during these 5 iterations.

3.4.3 How to enrich the disciplinary GPs?

One can note that to enrich a given disciplinary GP, let's say $\tilde{Y}_i$, it is necessary to provide a point in the space $\mathcal{Z} \times C^{(i)}$ where the disciplinary solver $f_i(z, y_{c^{(i)}})$ must be evaluated. However the method described so far only provides a point $z^{(new)} \in \mathcal{Z}$. In order to define the corresponding point $y_{c^{(i)}}^{(new)}$ it is proposed to solve the MDA using the mean values of the disciplinary GPs at point $z^{(new)}$, the obtained solution is thus used as $y_{c^{(i)}}^{(new)}$. It is interesting to note that, a large error on the MDA solution can be observed using this approach (as commented on Fig. 3) leading to a large error on the enrichment point $y_{c^{(i)}}^{(new)}$, however the uncertainty reduction algorithm depicted in Algo. 1 is designed to iteratively decrease this error until a relevant MDA solution is obtained. As an example, over the 5 iterations of Algo. 1 used on the 1-D toy example, 2 iterations have been performed at $z = -3.5$, 2 iterations at $z = -2.5$ and 1 iteration at $z = 3.7$.

Figure 12 illustrates on the 1-D toy example how the disciplinary GPs enrichment leads to a reduction of the uncertainty of the random MDA solution. Illustration is provided for the first two iterations of Algo. 1 at $z^{(new)} \approx -3.5$.

3.5 Proposed algorithm and exploitation of the results

The proposed algorithm for Efficient Global Multidisciplinary Optimization is now presented. It consists in coupling the two-step of enrichment previously introduced in an iterative process. Algorithm 2 summarizes the proposed approach.

One can note that the convergence of the proposed algorithm is not led by an accuracy criterion but by a budget limitation. However, after a given number of iterations, the value of the EI defined by Eq. (16) is

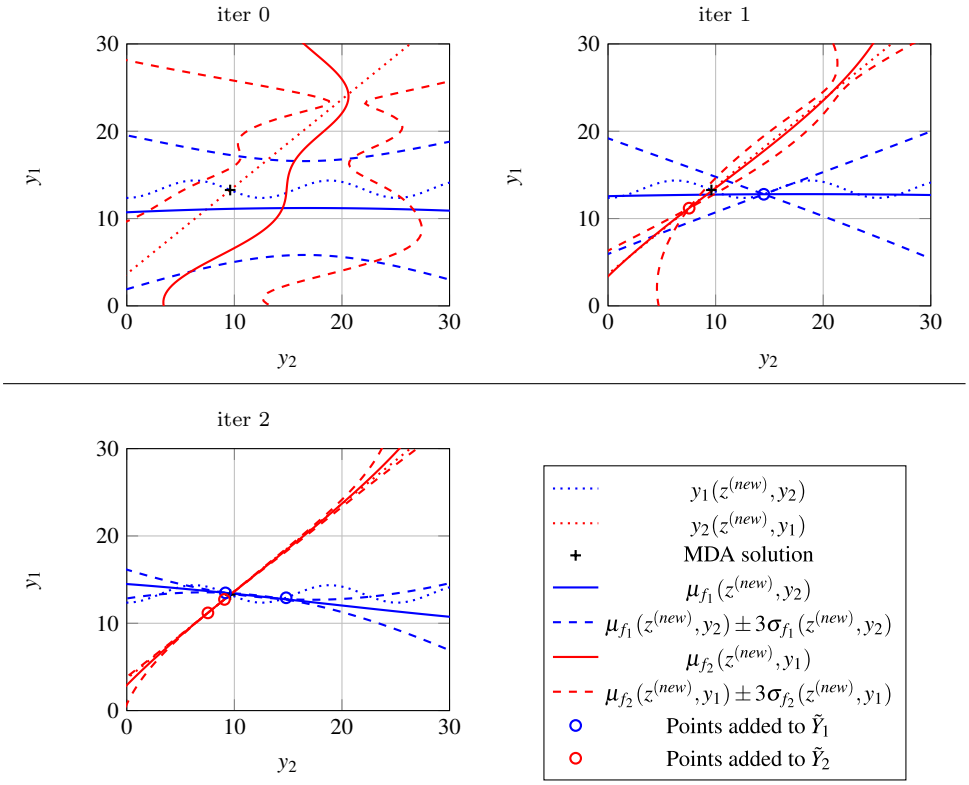

Fig. 12 1-D toy problem. Enrichment of the disciplinary GPs and uncertainty reduction on the random MDA solution $(\tilde{Y}_1^\star, \tilde{Y}_2^\star)$ during the first iterations of Algo. 1.

initialization: $\forall i \in n_d$, create DoE_{f_i} by sampling the disciplinary solver f_i over $\mathcal{Z} \times C^{(i)}$
$\forall i \in n_d$, create the disciplinary GPs, $\tilde{Y}_i$ (see Eq. (5))
Create the DoE_{UQ} by sampling over $\mathcal{Z}$
$\forall z^{(j)} \in \text{DoE}_{UQ}$ compute the PCE approximation $\hat{Y}_{obj}(z^{(j)}, \Xi)$ (see Eq. (12))
while $n_{iter} \leq n_{max}$ **do**
  $n_{iter} = n_{iter} + 1$
  Compute the mean vector and the eigenvector of the KL decomposition of the objective function random vector $\hat{\mathbf{Y}}_{obj}$ (see Eq. (13))
  Compute the continuous approximation of the random objective function by KL-GP interpolation of the mean vector and of the eigenvectors previously computed (see Eq. (14))
  Optimize the EI from Eq. (17) to find $z^{(new)}$
  Add $z^{(new)}$ to DoE_{UQ}
  Execute Algo. 1 to enrich the disciplinary GP if needed
end

Algorithm 2: Proposed Efficient Global MultiDisicplinary Optimization algorithm (EGMDO).

expected to be very low, which means that the possible improvement on the random variable $\hat{Y}_{min}^{(obj)}(\Xi)$ by adding a new discretization point is negligible. This translates the fact that the random field representation $\tilde{Y}_{obj}(z, \Xi, \eta)$, given by Eq. (14), reaches an acceptable accuracy in the areas of $\mathcal{Z}$ where the minimum is likely to be and consequently that in these areas the dispersion of the random field due to both disciplinary GP interpolation uncertainty (modeled by the Ξ random variable) and the KL-GP interpolation uncertainty (modeled by the η random variable) is negligible. Hence, we propose to use the mean value of the KL-GP interpolation in the random field representation given by Eq. (14) leading to

$$\hat{Y}_{obj}(z, \Xi) \approx \tilde{Y}_{obj}(z, \Xi) = \mu_{\tilde{\mu}_{\hat{\mathbf{Y}}_{obj}}}(z) + \sum_{k=1}^{n_{UQ}} \left(\sum_{i=2}^{P} \mathbf{a}_i^t \hat{\varphi}_k \phi_i(\Xi) \right) \mu_{\tilde{\varphi}_k}(z) \tag{19}$$

where $\mu_{\tilde{\mu}_{\hat{\mathbf{Y}}_{obj}}}(z)$ and $\mu_{\tilde{\varphi}_k}(z)$ are respectively the mean value of the KL-GP interpolation of the mean vector $\mu_{\hat{\mathbf{Y}}_{obj}}$ and of the eigenvectors $\hat{\varphi}_k$.

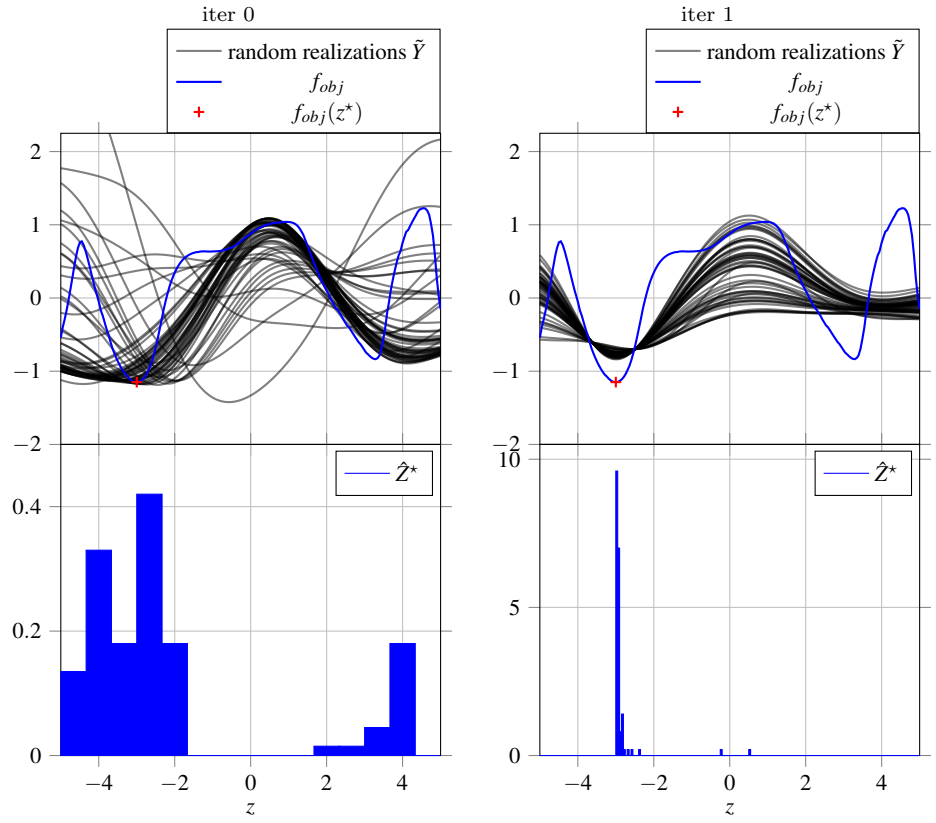

Fig. 13 1-D toy problem. 100 random samples of the model given by Eq. (19) and corresponding histograms of $\hat{Z}^\star$ given by Eq. (21) before and after the first iteration of Algo. 2 to illustrate the random position of the minimum.

Then, Eq. (19) can be seen as a metamodel of the random field modelling the objective function optimized to be accurate in the areas of $\mathcal{Z}$ where the minimum is likely to be. As a consequence it will be used in the following to estimate the probability distribution of the random variables modeling the minimum value of the objective function and its position such as,

$$\hat{Y}_{min}^{(obj)}(\Xi) = \min_{z\in\mathcal{Z}} \left(\hat{Y}_{obj}(z,\Xi)\right) \approx \min_{z\in\mathcal{Z}} \left(\tilde{Y}_{obj}(z,\Xi)\right) \tag{20}$$

and

$$\hat{Z}^\star(\Xi) = \arg\ \min_{z\in\mathcal{Z}} \left(\hat{Y}_{obj}(z,\Xi)\right) \approx \arg\ \min_{z\in\mathcal{Z}} \left(\tilde{Y}_{obj}(z,\Xi)\right) \tag{21}$$

Moreover, it should be noted that the random field representation given by Eq. (19) only involves polynomial functions and thus makes the estimation of $\hat{Y}_{min}^{(obj)}(\Xi)$ and $\hat{Z}^\star(\Xi)$ easily accessible by the MC method *i.e.* solving the minimization problem of Eq. (20) for a large number of samples $\Xi^{(j)}$, $j = 1, \cdots, n_{sim}$. As an illustration Fig. 13 presents on the 1-D toy example some realizations of the model given by Eq. (19) before and after the first iteration of Algo. 2. Figure 13 also reports the corresponding histograms of the minimum value position of the objective function *i.e.* $\hat{Z}^\star(\Xi)$, obtained by 100 MC simulations. Finally Fig. 14 presents the histograms of the minimum value of the objective function *i.e* $\hat{Y}_{min}^{(obj)}(\Xi)$ before and after the first iteration of Algo. 2.

One can note that, after a single iteration of the proposed Algo. 2, the uncertainties around the area of the global deterministic minimum position and values are drastically reduced as shown by Fig. 13 and Fig. 14. We recall that the point $z \approx -3.5$ is added to DoE_{UQ} and that 5 points are added to the disciplinary GPs by Algo. 1 (2 at $z \approx -3.5$, 2 at $z = -2.5$ and 1 at $z = 3.7$). On this simple 1-D toy example, one can see that after this single iteration of Algo. 2 the location of the minimum is almost perfectly identified, however a significant error still remains on the value of the minimum. The following 4 iterations of Algo. 2 only performed uncertainty quantification at points $z \approx -2.95$, $z = 5$, $z \approx 1.89$, $z = -5$ but without enrichment of the disciplinary GPs (and thus no call to the disciplinary solvers) and leads to the results presented in Fig. 15 showing that convergence to the global minimum is reached. Figure 16 presents the

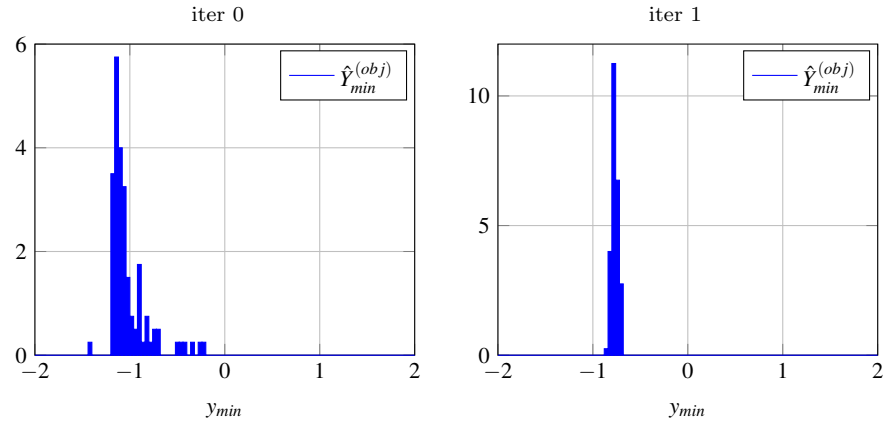

Fig. 14 1-D toy problem. Histograms of $\hat{Y}_{min}^{(obj)}$ given by Eq. (20) before and after the first iteration of Algo. 2 to illustrate the random value of the minimum.

corresponding histogram of $\hat{Y}_{min}^{(obj)}(\Xi)$ that shows the convergence towards the deterministic minimum value. It is important to note on Fig. 15 that the surrogate model of the objective function is only accurate in the vicinity of the global optimum since this was our stated goal. It is also important to recall, that unlike in classical EGO-type algorithms, the accuracy of the surrogate of the objective function in the vicinity of the global optimum was not only obtained by enrichment of this surrogate in the design variables space but also through enrichment of the disciplinary surrogate models.

A flowchart summarizing the proposed EGMDO approach is provided in Fig. 17 as well as a XDSM diagram in Appendix (see Fig. 26).

Next section provides a numerical study of the proposed approach on a classical benchmark MDO problem and on an engineering example.

4 Applications

4.1 A mathematical example

4.1.1 Presentation of the test case

The proposed EGMDO method is now applied on a test case derived from the one proposed in [28]. Compared to the original test case which is a constrained MDO problem counting one local and one global minima, the proposed test case is unconstrained but still counts one local and one global minima. It it defined by the following set of equations,

$$f_{obj}(z, y^\star_{c^{(obj)}}) = z_1 + z_3^2 + y_1^\star + \exp(-y_2^\star) + 10\cos(z_2)$$

where $z = \{z_1, z_2, z_3\}$, $c^{(obj)} = \{1, 2\}$ and $y^\star = \{y_1^\star, y_2^\star\}$ is solution of the following MDA, $\forall z \in \mathcal{Z}$,

$$\begin{aligned} y_1 &= f_1(z, y_2) = z_1 + z_2^2 + z_3 - 0.2y_2 \\ y_2 &= f_2(z, y_1) = \sqrt{y_1} + z_1 + z_2 \end{aligned}$$

Design space is defined by $\mathcal{Z} = [0, 10] \times [-10, 10] \times [0, 10]$.

Reference solution is obtained by using MDF approach with SLSQP optimization algorithm and leads to $z^\star \approx \{0, 2.634, 0\}$, $f_{obj}(z^\star) \approx -2.808$. Figure 18 presents the variation of f_{obj} in the plan (z_2, z_3) with $z_1 = 0$. It should be noted that the local minimum is located at $z^{lm} \approx \{0, -2.595, 0\}$ and leads to $f_{obj}(z^{lm}) \approx -0.809$.

4.1.2 Running EGMDO algorithm

In order to set up the proposed approach the following initial guess for the coupling variables spaces is proposed, $C^{(1)} = [-5, 24]$ and $C^{(2)} = [1, 50]$. It should be noted that choosing the initial guess for the coupling variables spaces is one of the drawback of the proposed approach. However, in a realistic case one

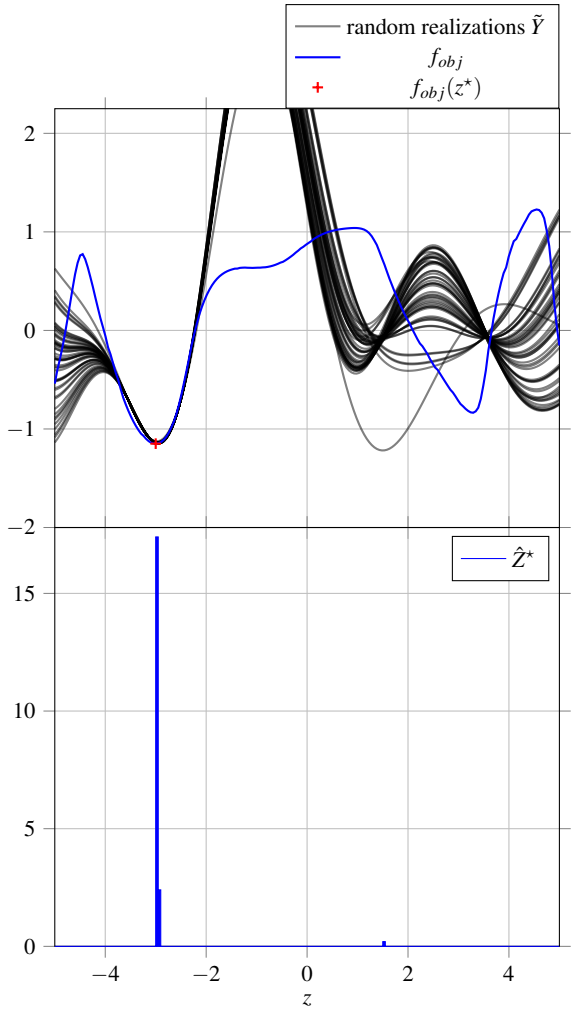

Fig. 15 1-D toy problem. 100 random samples of the model given by Eq. (19) and corresponding histograms of $\hat{Z}^\star$ given by Eq. (21) after 5 iterations of Algo. 2 to illustrate the random position of the minimum.

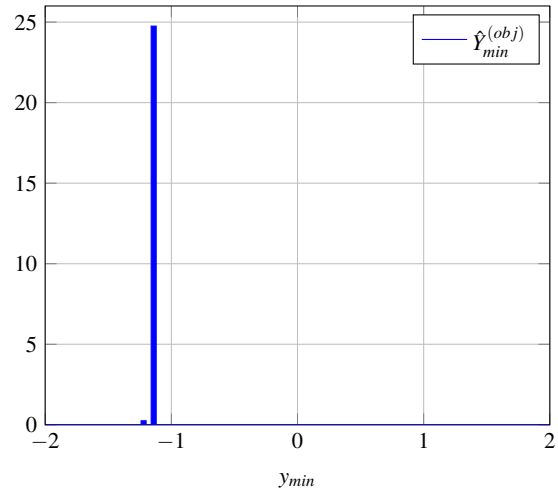

Fig. 16 1-D toy problem. Histograms of $\hat{Y}_{min}^{(obj)}$ given by Eq. (20) after 5 iterations of Algo. 2 to illustrate the random value of the minimum.

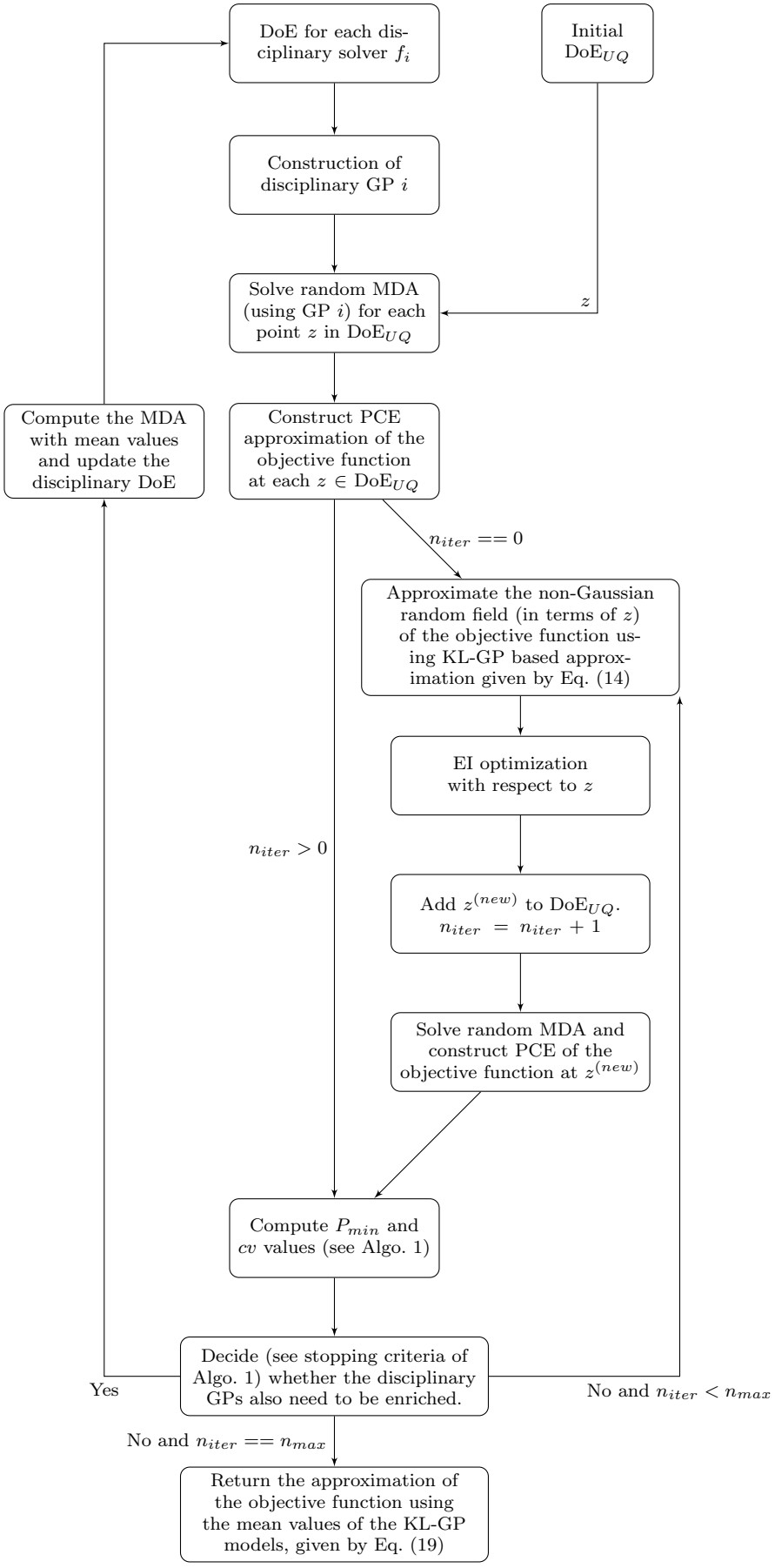

Fig. 17 Flowchart of the EGMDO algorithm.

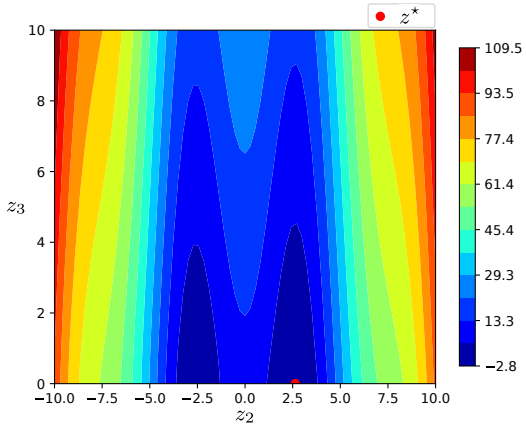

Fig. 18 Application problem. Variation of f_{obj} in the plan (z_2, z_3) with $z_1 = 0$ and location of the global minimum $z^\star$.

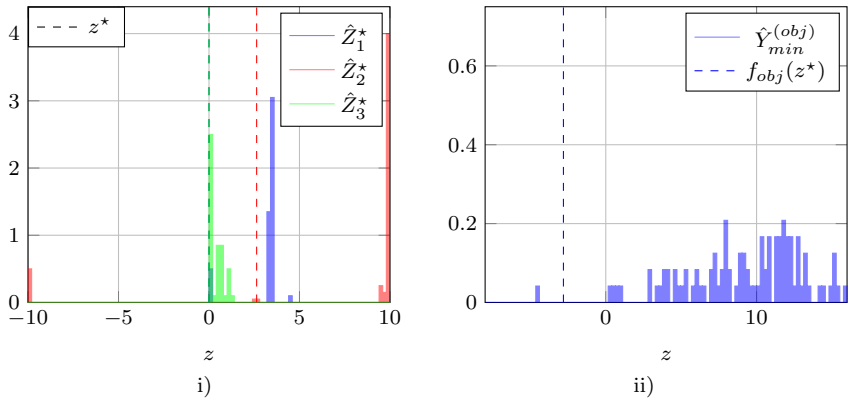

Fig. 19 Application example. i) Histograms of the minimum value position $\hat{Z}^\star$ ii) Histogram of the minimum value $\hat{Y}_{min}^{(obj)}$ at initialization of Algo. 2.

can rely on expert judgment to get a first approximation and, more importantly, Algo. 1 is designed to enrich these coupling spaces in promising areas without any limitation. As a consequence the boundaries of the coupling variables spaces might evolve during the iterations of Algo. 2 and thus a poor initial choice for these boundaries might lead to some extra iterations but should not be detrimental to the global convergence.

The initial disciplinary DoEs, DoE_{f_1} and DoE_{f_2}, count 5 points, respectively sampled by Latin Hypercube Sampling (LHS) over $\mathcal{Z} \times C^{(1)}$ and $\mathcal{Z} \times C^{(2)}$. Initial disciplinary GPs are then constructed using these DoEs and constant mean function and Gaussian covariance function are used. According to the proposed method the objective function is represented by a random field over $\mathcal{Z}$. The initial DoE_{UQ}, used to discretized this random field, counts 20 points sampled by LHS over $\mathcal{Z}$. Hence, uncertainty propagation by PCE is carried out at 20 points, PCE of degree 3 is retained and computation of the PCE coefficients is obtained by regression over 100 points. It should be noted that thanks to the approximation exposed in Section 3.2, the stochastic dimension of these uncertainty quantification problems is only 2 (*i.e.* $\Xi = \{\xi_1, \xi_2\}$), thus 100 regression points are large enough to compute the 10 unknown PCE coefficients by ordinary least square. We also recall that the regression sample of size 100 is obtained by solving non linear systems given by Eq. (9) only involving disciplinary GPs and thus having a negligible numerical cost.

At this initial stage, the approximation given by Eq. (19) is used to computed the approximation of the random variable modeling the position of the minimum ($\hat{Z}^\star$ given by Eq. (21)) and the random variable modeling the value of the minimum ($\hat{Y}_{min}^{(obj)}$ given by Eq. (20)). Figure 19 presents the results where histograms are obtained by 100 MC simulations using the model defined by Eq. (19).

Figure 19 shows that at initialization the position of the global minimum (Fig. 19 i)) as well as its value (Fig. 19 ii)) are poorly predicted by the model given by Eq. (19). Indeed the mean value of the random position of the minimum $\hat{Z}^\star$ is far from the reference one and its variance is quite large and consequently

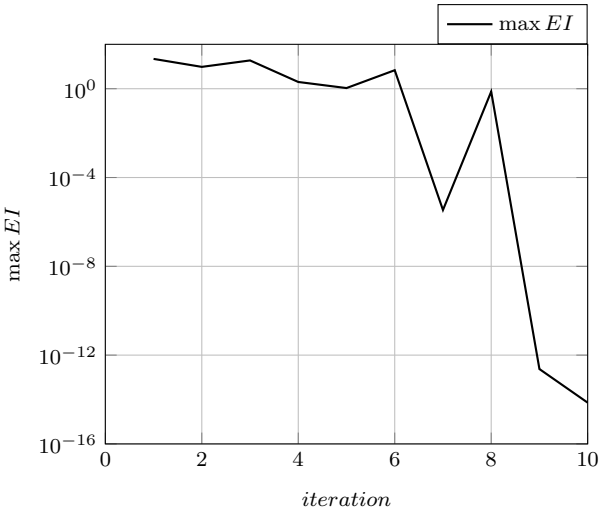

Fig. 20 Application example. Evolution of the maximum value of the EI defined by Eq. (16) with respect to the number of iterations of the proposed EGMDO algorithm.

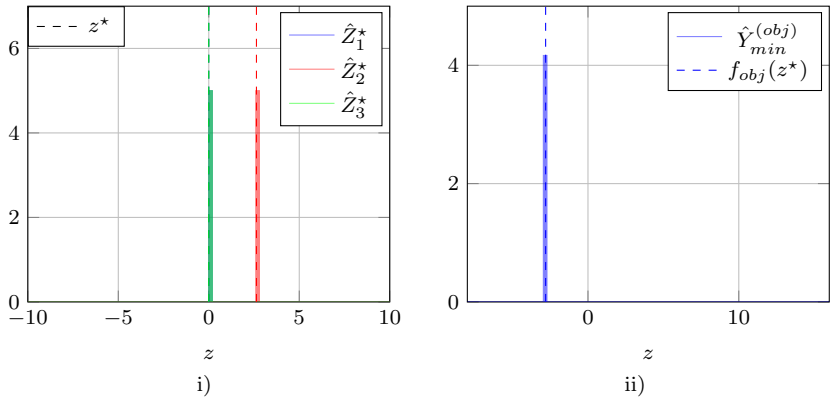

Fig. 21 Application example. i) Histograms of the minimum value position $\hat{Z}^\star$ ii) Histogram of the minimum value $\hat{Y}_{min}^{(obj)}$ after 10 iterations of Algo. 2.

the random minimum value of the objective function $\hat{Y}_{min}^{(obj)}$ presents a large variation. Objective of the proposed approach is to increase the accuracy of the model given by Eq. (19) by improving the disciplinary GPs only where the minimum is likely to be.

On this example the maximum number of iterations of Algo. 2 is set to $n_{max} = 10$ and the parameter ϵ_{cv} defined in Algo. 1 is set $\epsilon_{cv} = 0.01$. During these 10 iterations, 6 points are added to the disciplinary GPs by Algo. 1 which leads to a number of disciplinary solver evaluations equal to $5 + 6 = 11$. At final iteration the number of modes kept in the KL decomposition is $M = 6$.

Figure 20 presents the evolution of the maximum value of the EI defined by Eq. (16) with respect to the iterations of Algo. 2. As expected the maximum value of the EI is globally decreasing during iterations. Hence the uncertainty about the minimum value and position of the minimum of f_{obj} is reduced during iterations of the proposed optimization algorithm Algo. 2.

Figure 21 illustrates this uncertainty reduction and presents the histograms of $\hat{Z}^\star$ and $\hat{Y}_{min}^{(obj)}$ obtained after 10 iterations of Algo. 2. Histograms are still obtained by 100 MC simulations using the model defined by Eq. (19).

Compare to Fig. 19 one can note on Fig. 21 that the proposed algorithm reaches its objective after 10 iterations as the random minimum position $\hat{Z}^\star$ is almost multi-Dirac distributed and the three modes are in perfect agreement with the reference values. Concerning the random minimum value $\hat{Y}_{min}^{(obj)}$ the obtained probability distribution is also very close to a Dirac in perfect agreement with the reference value. In order to quantify the quality of the approximation provided by Algo. 2, Table 1 presents the mean values, the coefficients of variation and the relative errors (denoted by ϵ_{rel}) between the mean values and the reference ones for $\hat{Z}^\star$ and $\hat{Y}_{min}^{(obj)}$. The results presented by Table 1 confirm that the mean values of $\hat{Z}^\star$ and $Y_{min}^{(obj)}$

variables	$\hat{Z}_1^\star$	$\hat{Z}_2^\star$	$\hat{Z}_3^\star$	$\hat{Y}_{min}^{(obj)}$
$\mathbb{E}$	$\leqslant 10^{-12}$	2.634	$\leqslant 10^{-12}$	-2.798
cv	1.35	2.97×10^{-3}	3.52	1.11×10^{-2}
ϵ_{rel}		$\leqslant 0.01\%$		0.36%

Table 1 Application example. Mean values, coefficients of variation and relative errors between the mean values and the reference values for $\hat{Z}^\star$ and $\hat{Y}_{min}^{(obj)}$ obtained with the model given by Eq. (19) after 10 iterations of Algo. 2.

variables	$\hat{Z}_1^\star$	$\hat{Z}_2^\star$	$\hat{Z}_3^\star$	$\hat{Y}_{min}^{(obj)}$
$\mathbb{E}$	$\leqslant 10^{-12}$	2.631	5.38×10^{-4}	-2.822
cv	1.122×10^{1}	6.063×10^{-3}	2.223×10^{1}	2.153×10^{-2}
ϵ_{rel}		0.11%		0.49%

Table 2 Application example, robustness study. Mean values, coefficients of variation and relative errors between the mean values and the reference values for $\hat{Z}^\star$ and $\hat{Y}_{min}^{(obj)}$ obtained with the model given by Eq. (19) after 10 iterations of Algo. 2 over 7 initial DoEs.

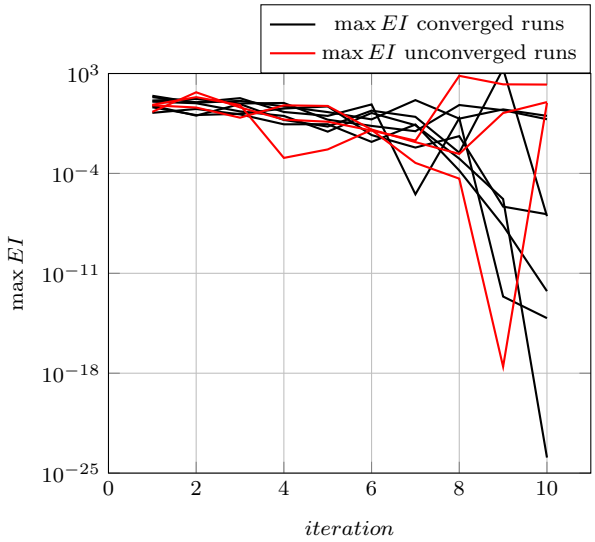

Fig. 22 Application example, robustness study. Evolution of the maximum value of the EI defined by Eq. (16) with respect to the number of iteration of the proposed EGMDO algorithm for 10 different initial DoEs.

are in perfect agreement with the reference ones. Moreover the coefficients of variation for $\hat{Z}_2^\star$ and $Y_{min}^{(obj)}$ are very low which confirms that the obtained probability distributions are almost Dirac. Concerning the large coefficient of variation for $\hat{Z}_1^\star$ and $\hat{Z}_3^\star$, it should be noted that this is due to the quasi null mean values and that the random variables $\hat{Z}_1^\star$ and $\hat{Z}_3^\star$ have however, in absolute, a very low dispersion.

4.1.3 Robustness study

Effect of randomness on the proposed approach is first assessed by running the previously introduced example on 10 different initial DoEs (DoE_{f_1}, DoE_{f_2}, DoE_{UQ}). The proposed EGMDO approach converged towards the global optimum 7 times. The mean number of points added to the disciplinary GP is 7 (minimum is 5 and maximum 11) leading to a mean number of disciplinary solver evaluations equal to $5 + 7 = 12$. The mean number of KL modes at last iteration is $M = 5$ (minimum is 5 and maximum is 6). For the 7 converged runs the mean values and coefficients of variation are estimated using 100 MC simulations and Table 2 presents the associated mean values over the 7 runs.

Results presented by Table 2 allow to conclude that the 7 runs of Algo. 2 that converge towards the global optimum achieve it with an excellent accuracy with respect to the reference value. It is now proposed to focus on the 3 runs that does not converge. First of all, Fig. 22 presents the evolution of the EI for the 10 runs and highlights the 3 runs that do not converged.

One can note on Fig. 22 that the 3 unconverged runs are the ones with the highest EI values at the last iteration of Algo. 2. This confirms the capability of the EI criterion to give valuable information on the accuracy of the approximation given by Eq. (14). It should be noted that this interpretation is also

variables	$\hat{Z}_1^\star$	$\hat{Z}_2^\star$	$\hat{Z}_3^\star$	$\hat{Y}_{min}^{(obj)}$
$\mathbb{E}$	0.626	-0.432	0.381	-34.306
cv	2.524	6.258	4.683	2.831

Table 3 Application example, robustness study. Mean values and coefficients of variation for $\hat{Z}^\star$ and $\hat{Y}_{min}^{(obj)}$ obtained with the model given by Eq. (19) after 10 iterations of Algo. 2 over the 3 runs that does not converged.

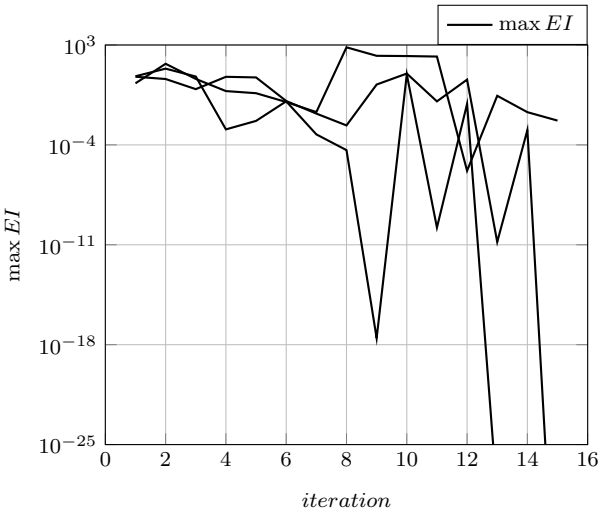

Fig. 23 Application example, robustness study. Evolution of the maximum value of the EI for the 3 previously unconverged runs after 15 iterations of Algo. 2.

run	EI	$\mathbb{E}(\hat{Z}_1^\star)$	$cv(\hat{Z}_1^\star)$	$\mathbb{E}(\hat{Z}_2^\star)$	$cv(\hat{Z}_2^\star)$	$\mathbb{E}(\hat{Z}_3^\star)$	$cv(\hat{Z}_3^\star)$	$\mathbb{E}(\hat{Y}_{min}^{(obj)})$	$cv(\hat{Y}_{min}^{(obj)})$
#1	$\leqslant 10^{-12}$	$\leqslant 10^{-12}$	2.95	2.636	2.80×10^{-3}	$\leqslant 10^{-12}$	3.33	-2.809	9.37×10^{-4}
#2	$\leqslant 10^{-12}$	$\leqslant 10^{-12}$	2.20	2.636	1.48×10^{-3}	$\leqslant 10^{-12}$	3.19	-2.808	9.22×10^{-4}
#3	5.05×10^{-3}	6.601×10^{-1}	9.91×10^{-3}	-3.767	3.20×10^{-2}	4.671×10^{-1}	7.09×10^{-2}	-10.751	1.49×10^{-1}

Table 4 Application example, robustness study. Final value of the EI, mean values and coefficients of variation of $\hat{Z}^\star$ and $\hat{Y}_{min}^{(obj)}$ obtained on the 3 previously unconverged runs after 15 iterations of Algo. 2.

confirmed by estimating the standard deviation values of $\hat{Z}_2^\star$ and $\hat{Y}_{min}^{(obj)}$ which are very high compared to the one obtained on the converged runs. Table 3 reports these values.

In order to improve the accuracy of the 3 unconverged runs, the maximum number of iterations of Algo. 2 is set to 15. Note that 5 iterations are added to the previous runs. Figure 23 presents the maximum value of the EI during the 15 iterations of Algo. 2 for the 3 previously unconverged runs. One can note that this time, at last iteration, the values reached by EI are very low (especially true for 2 runs, the third one equals 5×10^{-3}). These results seem to show that adding 5 iterations allows Algo. 2 to converge for these 3 previously unconverged runs. Table 4 details the results for the 3 runs. First it is notable that, for the 3 runs, the probability distributions of $\hat{Z}^\star$ and $\hat{Y}_{min}^{(obj)}$ almost converged to Dirac distributions according to the low coefficients of variation. However only runs #1 and #2 converge towards the global optimum with a high accuracy compared to the reference results. It should be added that the number of points added to the disciplinary DoEs during the 15 iterations of Algo. 2 for these 2 runs is respectively equal to 7 and 6.

The run #3 converges towards a fake minimum as the minimum value obtained (-10.751) is lower than the reference one. This behavior shows that the approximation of the objective function given by Eq. (19) is of poor quality. Our explanation is that, for this particular DoE_{UQ}, the approximation obtained by Eq. (19) is probably highly oscillating which is a well known problem in Gaussian process interpolation. Moreover, it should be added that for sake of simplicity only squared exponential correlation function has been used and it is also well known that this correlation function can lead to numerical instability. Improving the result by testing others correlation function should be seen as a perspective of this work.

Based on these results a robustness study over 100 runs is now performed still using initial disciplinary DoE of size 5, DoE_{UQ} of size 20 and 15 iterations of Algo. 2. After 15 iterations, 88 runs converged towards the global optimum. It should be noted that a run is considered as convergent if the relative error between the estimated mean value of $\mathbb{E}(\hat{Z}^\star)$ and the reference value is less than 5%. The mean number of points added to the disciplinary DoE during the 15 iterations of Algo. 2 is equal to 8, which leads to a mean

variables	$\hat{Z}_1^\star$	$\hat{Z}_2^\star$	$\hat{Z}_3^\star$	$\hat{Y}_{min}^{(obj)}$
$\mathbb{E}$	1.710×10^{-3}	2.625	1.338×10^{-13}	-2.788
cv	0.448	5.083×10^{-3}	2.987	3.895×10^{-3}
ϵ_{rel}		0.34%		0.71%

Table 5 Application example, robustness study. Mean values, coefficients of variation and relative errors between the mean values and the reference values for $\hat{Z}^\star$ and $\hat{Y}_{min}^{(obj)}$ obtained with the model given by Eq. (19) after 15 iterations of Algo. 2 over 88 initial DoE.

number of disciplinary solver evaluations equal to $5 + 8 = 13$. Table 5 summarizes the obtained results. As for Table 2 for each run the mean values and coefficients of variation are estimated using 100 MC simulations. The Table 5 presents the mean values over the 88 runs of these mean values and coefficients of variation.

Some comparisons with classical MDO formulations are now provided. More precisely the MDF and IDF formulations are used in conjunction with the following optimization algorithm:

- A gradient based algorithm namely SLSQP Sequential Least SQuares Programming [16] where gradient is estimated by finite differences,
- A gradient free algorithm namely COBYLA Constrained Optimization BY Linear Approximation [23],
- A surrogate based algorithm namely EGO Efficient Global Optimization [14] using either the Expected Improvement criterion (EI) or an alternative criterion denoted by WB2s (see [3] for the definition of WB2s criterion).

Resolution with SLSQP and COBYLA has been implemented using the python package scipy [15], resolution with EGO used an in house python implementation [3].

For each of these formulations 100 runs are performed with different starting point for SLSQP and COBYLA and different initial DoE for EGO (initial DoE of size 12 for the MDF-EGO and of size 20 for the IDF-EGO). Table 6 presents the number of runs that converged towards the global optimum (line n_{con}) and the mean number number of disciplinary solver evaluations over the n_{con} runs that converged (line n_{eval}).

	MDF-SLSQP	MDF-COBYLA	MDF-EGO-EI	MDF-EGO-WB2s	EGMDO
$n_{con}(\%)$	57	66	96	100	88
n_{eval}	197	638	296	212	13
	IDF-SLSQP	IDF-COBYLA	IDF-EGO-EI	IDF-EGO-WB2s	
$n_{con}(\%)$	56	70	99	100	
n_{eval}	68	206	63	44	

Table 6 Application example, comparative study. Results obtained with MDF and IDF formulations with 3 different optimizers (SLSQP, COBYLA, EGO with two criteria EI and WB2s). Number of converged runs and mean number of disciplinary solver evaluations are reported for each formulation over 100 runs. Results obtained by the proposed EGMDO approach are recalled in last column

Results provided by Table 6 allow to draw several conclusions:

- As expected, the number of evaluations of the disciplinary solvers is lower using the IDF approach than the MDF approach.
- Classical local optimization algorithms (gradient based SLSQP or gradient free COBYLA) have a poor convergence rate (between 56% and 70%) using either the MDF or the IDF formulation.
- Global surrogate based optimizer EGO reaches the best results in terms of convergence rate (between 96% and 100%). It is notable that both MDF and IDF formulations in conjunction with the WB2s criterion converge to the global optimum for every run.
- The best result is obtained using IDF formulation with EGO-WB2s as optimizer. This approach converges to the global optimum for every case with a mean number of disciplinary solver evaluations equals to 44 which is the lowest value on this comparison.
- Concerning the result obtained with the proposed EGMDO approach, one can note that the convergence rate of 88% is better than the one obtained using local optimizers but lower than the one obtained by EGO. However the mean number of disciplinary solver evaluations is only 13 for the EGMDO approach, compared to 44 for the IDF-EGO-WB2s. As a conclusion these results should be seen as promising for the new EGMDO approach as, even if it does not reach a 100% convergence rate, the benefit in terms of disciplinary solver evaluations is important.

4.2 A compound cylinder

4.2.1 Presentation of the test case

This test case is inspired by the one used in [12] and [7] and deals with a compound cylinder. Figure 24 presents the compound cylinder as well as the the two sub systems, the inner and outer cylinder respectively. Figure 24 also introduces the notations for the radii of the two cylinders (a, b, c) and the pressure inside the inner cylinder (P_0). It should be noted that this example does not involve two disciplines but rather two

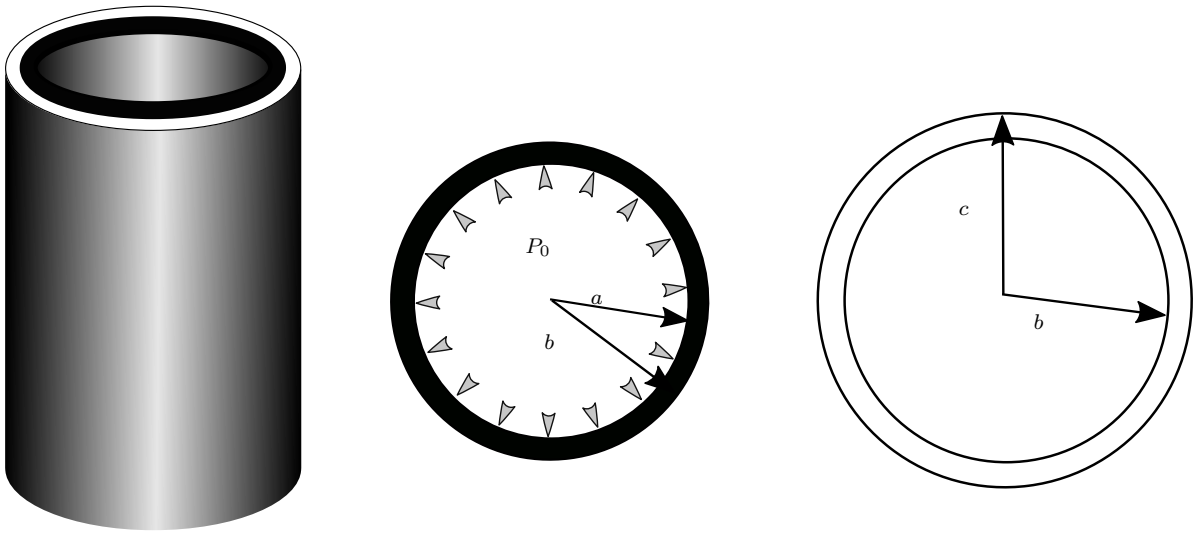

i) ii) iii)

Fig. 24 Compound cylinder test case. i) Compound cylinder ii) Inner cylinder iii) Outer cylinder

components coupled together. However the formalism of the problem is exactly the one of a multidisciplinary system as presented by Eq. (4). Indeed the two cylinders are coupled through the radial deformation of the inner cylinder δ_1 and the contact stress at the interface p. The MDA can thus be defined by the following system of two equations,

$$\begin{aligned} f_1(p) = \delta_1 &= \frac{pb}{E}\left(\frac{a^2+b^2}{b^2-a^2} - \rho\right) \\ f_2(\delta_1) = p &= \frac{(\delta-\delta_1)E}{b} \Big/ \left(\frac{b^2+c^2}{c^2-b^2} + \rho\right) \end{aligned} \tag{22}$$

where E is the elasticity modulus of the material of the two cylinders, ρ is the Poisson's ratio and δ is the allowable total shrinkage. Once the equilibrium is reached (*i.e.* the values $\delta_1^\star$ and $p^\star$ solving Eq. (22) have been determined) the distribution of tangential stress in the two cylinders can be computed by:

$$\sigma_\theta(r) = \begin{cases} A_1(p^\star) + \frac{B_1(p^\star)}{r}, \ r \in [a,b] \\ A_2(p^\star) + \frac{B_2(p^\star)}{r}, \ r \in [b,c] \end{cases} \tag{23}$$

where we have

$$\begin{aligned} B_1(p^\star) &= (\sigma_\theta^a(p^\star) - \sigma_\theta^{b-}(p^\star))\frac{a^2b^2}{a^2+b^2} \\ A_1(p^\star) &= \sigma_\theta^a(p^\star) - \frac{B_1(p^\star)}{a^2} \\ B_2(p^\star) &= (\sigma_\theta^{b+}(p^\star) - \sigma_\theta^c(p^\star))\frac{b^2c^2}{b^2+c^2} \\ A_2(p^\star) &= \sigma_\theta^{b+}(p^\star) - \frac{B_2(p^\star)}{2^2} \end{aligned}$$

and

$$\begin{aligned} \sigma_\theta^a(p^\star) &= \frac{-2p^\star b^2}{b^2-a^2} + \frac{(a^2+c^2)P_0}{c^2-a^2} \\ \sigma_\theta^{b-}(p^\star) &= \frac{-p^\star(b^2+a^2)}{b^2-a^2)} + \frac{a^2P_0(b^2+c^2)}{(b^2*(c^2-a^2))} \\ \sigma_\theta^{b+}(p^\star) &= p^\star\frac{b^2+c^2}{c^2-b^2} + \frac{a^2P_0(b^2+c^2)}{b^2(c^2-a^2)} \\ \sigma_\theta^c(p^\star) &= \frac{2b^2p^\star}{c^2-b^2} + \frac{2a^2P_0}{c^2-a^2} \end{aligned}$$

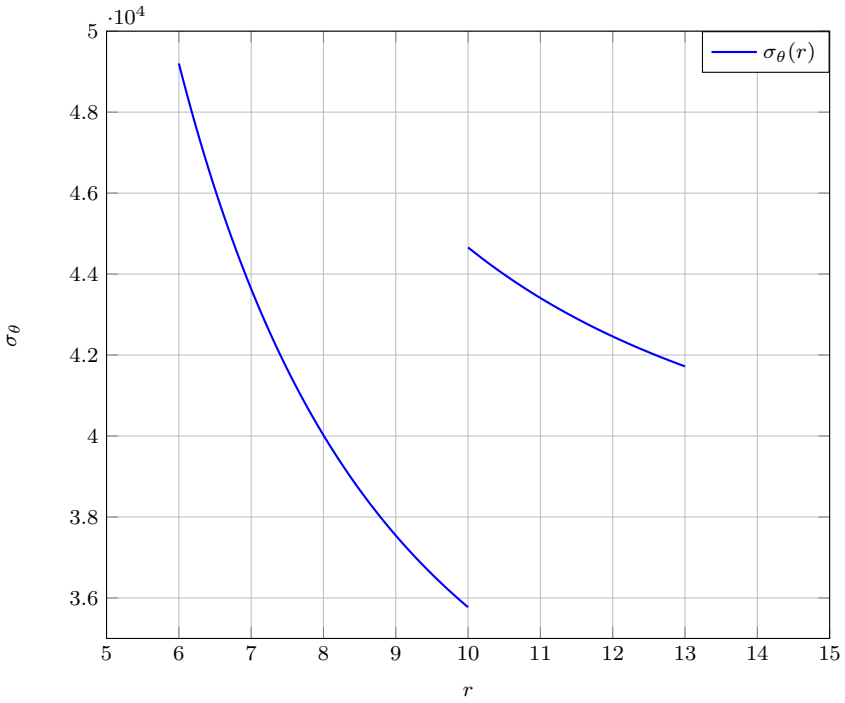

Fig. 25 Compound cylinder example, distribution of the tangential stress in the two cylinders with the initial configuration.

Figure 25 provides the plot of the tangential stress with respect to the radius using the following numerical values, $E = 3 \times 10^7$ psi, $\rho = 0.3$, $p_0 = 40000$ psi, $a = 6$ in, $b = 10$ in, $c = 13$ in and $\delta = 8 \times 10^{-3}$ in.

One can note on Fig. 25 that the tangential stress distribution in the two cylinders presents large variations in the first cylinder and between the two cylinders (discontinuity of the stresses). In the following an optimization problem whose objective is to reduce these variations is proposed. Consequently the following objective function is considered:

$$f_{obj}(z, y^\star_{c^{(obj)}}) = \frac{\sqrt{\mathbb{V}ar_r(\sigma_\theta(r, z, y^\star_{c^{(obj)}}))}}{\mathbb{E}_r(\sigma_\theta(r, z, y^\star_{c^{(obj)}}))} \tag{24}$$

where $\mathbb{E}_r$ and $\mathbb{V}ar_r$ respectively stand for the mean and variance with respect to the radius r. The design variables are $z = \{a, b, c, \delta\} \in \mathcal{Z} = [5, 7] \times [9, 11] \times [12, 15] \times [6 \times 10^{-3}, 10^{-2}]$, and $y^\star_{c^{(obj)}} = p^\star$ is solution of the MDA of Eq. (22).

The reference solution is obtained by an MDF approach using the SLSQP optimization algorithm. The following results are obtained $z^\star \approx \left\{7.00, 9.00, 12.00, 6.37 \times 10^{-3}\right\}$ and $f_{obj}(z, y^\star_{c^{(obj)}}) \approx 2.33 \times 10^{-2}$. It should be noted that using the initial configuration (the one used for Fig. 25, *i.e* $z^0 = \left\{6.00, 8.00, 11.00, 8.00 \times 10^{-3}\right\}$) leads to $f_{obj}(z^0, y^\star_{c^{(obj)}}) \approx 7.00 \times 10^{-2}$.

4.2.2 Application of EGMDO algorithm

In the following it is proposed to use this test case to study the influence of the initial disciplinary DoE size on the convergence of the EGMDO algorithm. Input of the first disciplinary analysis Eq. (22) is a vector of dimension $d_1 = 3$ containing the variables a, b, p, whereas input of the second disciplinary analysis is a vector of dimension $d_2 = 4$ containing the variables b, c, δ, δ_1. The performance of the EGMDO algorithm is evaluated using initial disciplinary DoE of size $d_i + 1$, $2d_i$, $3d_i$ or $4d_i$, $i = [1, 2]$. The initial guess for the coupling variable space is set to $\mathcal{C}^{(p)} = [1000, 9000]$ and $\mathcal{C}^{(\delta_1)} = [0, 6 \times 10^{-3}]$. As for the first example the initial DoE_{UQ} used to discretize the random field modeling the objective function, counts 20 points sampled by LHS over $\mathcal{Z}$. Hence, uncertainty propagation by PCE is carried out at 20 points, PCE of degree 3 is retained and computation of the PCE coefficients is obtained by regression over 100 points. The total number of iterations of the EGMDO algorithm is set to 20. Parameter ϵ_{cv} of Algo. 1 is still set to $\epsilon_{cv} = 0.01$.

For each disciplinary DoE size the mean and coefficient of variation of the minimum random position $\hat{Z}^\star$ and its value $\hat{Y}_{min}^{(obj)}$ are estimated with a sample of size 100 using the final objective function approximation given by Eq. (19). This operation is repeated 10 times for each disciplinary DoE size. Table 7 presents the number of converged runs for each size of disciplinary DoE over the 10 repetitions as well as the maximum, minimum, and mean number of points added to the disciplinary DoE, respectively denoted by n_{add}^+, n_{add}^- and n_{add} for the converged runs. So that the mean total number of disciplinary solver evaluations is the size of the initial disciplinary DoE plus n_{add} (line ($n_{(f_1,f_2)}$ in Table 7). As for the first example a run is considered as converged if the relative error between the estimated mean value of $\mathbb{E}(\hat{Z}^\star)$ and the reference value is less than 5%.

DoE_{f_i} size	d_i+1	$2d_i$	$3d_i$	$4d_i$
n_{con}	6	8	8	9
n_{add}^+	10	9	5	4
n_{add}^-	5	5	2	2
n_{add}	8	7	4	3
$n_{(f_1,f_2)}$	(12,13)	(13,15)	(13,16)	(15,19)

Table 7 Compound cylinder example. Number of converged runs n_{con} over 10 runs for different initial disciplinary DoE size.

It could be noted from the results of Table 7 that the initial DoE size of d_i+1 affects the performance of the proposed method. This shows that if the initial disciplinary GPs are not accurate enough, the exploratory phase of the algorithm will fail in finding the global minimum which is a classical problem in surrogate based optimization. However starting from the disciplinary size $2d_i$ the proposed approach reaches an acceptable level of converged runs on this example. Then, for DoE size $2d_i$, $3d_i$ or $4d_i$ it is interesting to note that the number of added points decreases with respect to the initial DoE size. This is not surprising as with a large initial DoE size the exploratory phase is shorten to directly focus on the interesting areas of the design space. Nevertheless it should be noted that even with a large initial disciplinary DoE the points added by the proposed method allows to get an accurate approximation of the objective function in the neighborhood of the minimum. To confirm this hypothesis, disciplinary surrogate models are constructed using $4d_i+n_{add}^+$ points (*i.e* GP of the first discipline is constructed from a DoE of size 16 drawn by LHS and the GP of the second discipline is constructed from a DoE of size 20 drawn by LHS). These two disciplinary GPs are then used to solve the problem with a MDF approach using SLSQP as optimizer. As for the proposed strategy 10 different disciplinary DoE are used. Over these 10 runs only 2 converged towards the correct minimum. This result clearly shows, on this example, the benefit and the relevance of the proposed adaptive enrichment strategy compared to a direct surrogate model based strategy.

5 Conclusions

This article presents the basis of a new adaptive surrogate based methodology to solve MDO problems. The main idea is to replace the numerically costly disciplinary solvers by GP surrogate models. As these GPs are constructed independently this approach allows to uncouple the MDA non linear problem, which can be advantageous in an industrial context. Moreover, in order to focus the computational budget on the optimization task, the disciplinary GPs are constructed adaptively, increasing their accuracy only where the minimum of the objective function is likely to be. Although this adaptive construction is classical when the objective function is modeled by a GP since the work by Jones [14], it represents a challenge in the proposed GP based MDO context. To solve this challenge, the present article proposed three developments. First a simplified disciplinary GP model is introduced in Section 3.2 which allows to efficiently estimate the uncertainty in the coupling variables by sampling. Second, it is proposed to model the objective function by a non Gaussian random field approximated by a hybrid PCE-KL-GP model defined in Section 3.3 by Eq. (14). Finally a two-step uncertainty reduction stage is proposed in Section 3.4. Objective of these uncertainty reduction steps is to enrich the disciplinary GPs until the uncertainty on the minimum of the objective function is negligible. The first step is designed to find the best point (with respect to the adapted Expected Improvement criterion) in the design space where the uncertainty quantification by PCE must be performed. Then, the second step uses the discretization of the random objective function by PCE to determine where in the design space the disciplinary GPs should be enriched. An iterative procedure

coupling these two steps is presented by Algo. 2. Finally, Section 4 presents numerical applications that confirm the interest of the proposed methodology in terms of number of disciplinary solver evaluations for the resolution of the global MDO problem. This Section also shows the potential ways of improvement of the proposed methodology. First, all the GPs used in the proposed approach use constant trend and squared exponential correlation function. According to our experiments (not shown in the article) a wise choice for these parameters can significantly improve the EGMDO approach. Second, Table 6 showed that the best convergence rate for the analytical application problem is obtained using a global optimizer and the WB2s criterion. As this criterion is a slight modification of the EI it could be interesting to investigate its behaviour on EGMDO. The optimization of the EI is also a difficult point. Indeed, optimization of this noisy function (expectation estimation by MC) is challenging and a dedicated algorithm such as stochastic gradient combined with multiple starting points can probably improve the approach or at least its numerical efficiency. These three improvements can be seen as short term perspectives. A more long term objective will be to study the sensitivity of the objective minimum with respect to the uncertainty introduced by the disciplinary GPs. Such a sensitivity analysis will benefit the enrichment step as it will allow to enrich only the disciplinary GP responsible for most of the variation of the objective minimum as in the current EGMDO approach all the disciplinary GPs are enriched during the iterative procedure. It should be noted that this idea has been developed by [12] in the context of reliability analysis. Finally, constraints handling should also be considered in the future. The simplest answer to this challenge is to construct surrogate models for the constraints and to optimize the EI with respect to these constraints. This strategy is adopted in Bayesian optimization with convincing results as in [3], [27].

Acknowledgements

This work was partially supported by the French National Research Agency (ANR) through the ReBReD project under grant ANR-16-CE10-0002 and by a ONERA internal project MUFIN dedicated to multi-fidelity. Part of the research presented in this paper has been performed in the framework of the AGILE 4.0 project (Towards Cyber-physical Collaborative Aircraft Development) and has received funding from the European Union Horizon 2020 Programme under grant agreement n^{o} 815122.

6 Replication of results

This section gives numerical details on the implementation of Algo.1 and Algo. 2. All the numerical results have been obtained using python 2.7.15 and the packages openTURNS 1.12 and numpy 1.15.4. In the following the default values of the algorithm provided by these packages are used expect if mentionned otherwise.

- The initial disciplinary DoE, denoted by DoE_{f_i} and the initial DoE for uncertainty quantification, denoted by DoE_{UQ} are sampled by Latin Hypercube Sampling (LHS) using the class `LHSExperiment` of openTURNS assuming uniform probability distributions between the lower and upper bounds.
- For the creation of the Gaussian processes (disciplinary GPs and KL-GP), all the input samples are centered and reduced. The GPs are constructed using the class `KrigingAlgorithm` of openTURNS, with constant trend (`ConstantBasisFactory` in openTURNS) and squared exponential correlation function (`SquaredExponential` in openTURNS). Optimization of the hyperparameters is performed by maximum likelihood. Range for the optimization is set to $[0.3, 100]$ for each hyperparameter (this choice avoids highly oscillating GP).
- The PCE are computed using the class `FunctionalChaosAlgorithm` of openTURNS. The polynomial basis is obtained by tenzorisation of the 1-D hermite polynomial basis. Coefficients of the PCE are computed by ordinary least square (`LeastSquaresStrategy`) in openTURNS, using a sample of size 100, sampled from an independent multinormal probability distribution of dimension n_d (as detailed in Section 4).
- Mean and covariance matrix of the PCE vector are obtained using the `FunctionalChaosRandomVector` of openTURNS. Eigenvalues and eigenvectors of the covariance matrix are computed with the command `eig` from the python toolbox `numpy.linalg`. The number of modes kept in the KL decomposition is defined such as the cumulative sum of the M highest eigenvalues is strictly higher than $1 - 10^{-6}$.
- As detailed in [9], the optimization of the EI (Eq. (17)) is performed using openTURNS class `OptimizationProblem`, with the COBYLA method with the parameter `RhoBeg` set to 0.5. It should be noted that all the inputs are normalized with a linear transformation from their respective range to $[0, 1]$ for the resolution of the

optimization problem. Finally 20 multiple starting points sampled uniformly are used to increase the chance of finding the global optimum of the EI.
– Resolution of the MDA for a given realization of the disciplinary GP (see Section 3.2) is performed by the non linear Jacobi method. The convergence condition is reached when the mean relative change in the coupling variables between two successive iterations is less than 10^{-6}. Note that the same algorithm and the same convergence condition are applied when the MDA is solved on the mean value of the disciplinary surrogate for enrichment purpose (see Section 3.4.2).

References

1. Arnst, M., Ghanem, R., Phipps, E., Red-Horse, J.: Dimension reduction in stochastic modeling of coupled problems. International Journal for Numerical Methods in Engineering **92**(11), 940–968 (2012). DOI 10.1002/nme.4364. URL http://dx.doi.org/10.1002/nme.4364
2. Azaïs, J.M., Wschebor, M.: On the roots of a random system of equations. The theorem of Shub and Smale and some extensions. Foundations of Computational Mathematics **5**(2), 125–144 (2005). DOI 10.1007/s10208-004-0119-0. URL https://doi.org/10.1007/s10208-004-0119-0
3. Bartoli, N., Lefebvre, T., Dubreuil, S., Olivanti, R., Priem, R., Bons, N., Martins, J., Morlier, J.: Adaptive modeling strategy for constrained global optimization with application to aerodynamic wing design. Aerospace Science and Technology **90**, 85 – 102 (2019). DOI https://doi.org/10.1016/j.ast.2019.03.041. URL http://www.sciencedirect.com/science/article/pii/S1270963818306011
4. Berveiller, M., Sudret, B., Lemaire, M.: Stochastic finite elements: a non-intrusive approach by regression. European Journal of Computational Mechanics **15**(1-3), 81 – 92 (2006)
5. Chen, X., Wang, P., Zhang, D.: Surrogate-based multidisciplinary design optimization of an autonomous underwater vehicle hull. In: 2017 16th International Symposium on Distributed Computing and Applications to Business, Engineering and Science (DCABES), pp. 191–194 (2017). DOI 10.1109/DCABES.2017.48
6. Cramer, E., Dennis Jr., J., Frank, P., Lewis, R., Shubin, G.: Problem formulation for multidisciplinary optimization. SIAM Journal on Optimization **4**(4), 754–776 (1994). DOI 10.1137/0804044. URL https://doi.org/10.1137/0804044
7. Du, X., Guo, J., Beeram, H.: Sequential optimization and reliability assessment for multidisciplinary systems design. Structural and Multidisciplinary Optimization **35**(2), 117–130 (2008). DOI 10.1007/s00158-007-0121-7. URL https://doi.org/10.1007/s00158-007-0121-7
8. Dubreuil, S., Bartoli, N., Gogu, C., Lefebvre, T.: Propagation of modeling uncertainty by polynomial chaos expansion in muldisciplinary analysis. Journal of Mechanical Design **138**(11), 111,411 (2016). DOI 10.1115/1.4034110
9. Dubreuil, S., Bartoli, N., Gogu, C., Lefebvre, T., Colomer, J.M.: Extreme value oriented random field discretization based on an hybrid polynomial chaos expansion - kriging approach. Computer Methods in Applied Mechanics and Engineering **332**, 540 – 571 (2018). DOI https://doi.org/10.1016/j.cma.2018.01.009. URL http://www.sciencedirect.com/science/article/pii/S0045782517302736
10. Dubreuil, S., Bartoli, N., Lefebvre, T., Gogu, C.: Efficient global multidisciplinary optimization based on surrogate models. In: 2018 Multidisciplinary Analysis and Optimization Conference, p. 3745 (2018)
11. Ghanem, R.G., Spanos, P.D.: Stochastic finite elements: a spectral approach. Springer, New York, NY (1991)
12. Hu, Z., Mahadevan, S.: Adaptive Surrogate Modeling for Time-Dependent Multidisciplinary Reliability Analysis. Journal of Mechanical Design **140**(2) (2017). DOI 10.1115/1.4038333. URL https://doi.org/10.1115/1.4038333. 021401
13. Jiang, Z., Li, W., Apley, D.W., Chen, W.: A spatial-random-process based multidisciplinary system uncertainty propagation approach with model uncertainty. Journal of Mechanical Design **137**(10), 101,402 (2015)
14. Jones, D.R., Schonlau, M., Welch, W.J.: Efficient global optimization of expensive black-box functions. Journal of Global Optimization **13**(4), 455–492 (1998). DOI 10.1023/A:1008306431147. URL http://dx.doi.org/10.1023/A:1008306431147
15. Jones, E., Oliphant, T., Peterson, P., et al.: SciPy: Open source scientific tools for Python (2001–). URL http://www.scipy.org/
16. Kraft, D.: A software package for sequential quadratic programming. Tech. Rep. DFVLR-FB–88-28, DLR German Aerospace Center – Institute for Flight Mechanics, Koln, Germany (1988)
17. Lambe, A.B., Martins, J.R.R.A.: Extensions to the design structure matrix for the description of multidisciplinary design, analysis, and optimization processes. Structural and Multidisciplinary Optimization **46**, 273–284 (2012). DOI 10.1007/s00158-012-0763-y
18. Liu, Y., Shi, Y., Zhou, Q., Xiu, R.: A sequential sampling strategy to improve the global fidelity of metamodels in multilevel system design. Structural and Multidisciplinary Optimization **53**(6), 1295–1313 (2016). DOI 10.1007/s00158-015-1379-9. URL https://doi.org/10.1007/s00158-015-1379-9
19. Martins, J.R., Alonso, J.J., Reuther, J.J.: A coupled-adjoint sensitivity analysis method for high-fidelity aero-structural design. Optimization and Engineering **6**(1), 33–62 (2005)
20. Martins, J.R.R.A., Lambe, A.B.: Multidisciplinary Design Optimization: A Survey of Architectures. AIAA Journal **51**(9), 2049–2075 (2013). DOI 10.2514/1.J051895. URL http://dx.doi.org/10.2514/1.J051895
21. Paiva, R.M., D. Carvalho, A.R., Crawford, C., Suleman, A.: Comparison of surrogate models in a multidisciplinary optimization framework for wing design. AIAA Journal **48**(5), 995–1006 (2010). DOI 10.2514/1.45790. URL https://doi.org/10.2514/1.45790
22. Picheny, V., Wagner, T., Ginsbourger, D.: A benchmark of kriging-based infill criteria for noisy optimization. Structural and Multidisciplinary Optimization **48**(3), 607–626 (2013)
23. Powell, M.J.D.: Direct search algorithms for optimization calculations. Acta Numerica **7**, 287–336 (1998). DOI 10.1017/S0962492900002841
24. Rasmussen, C.E., Williams, C.K.I.: Gaussian processes for machine learning. Adaptive computation and machine learning. MIT Press, Cambridge, Mass (2006)

25. Sankararaman, S., Mahadevan, S.: Likelihood-Based Approach to Multidisciplinary Analysis Under Uncertainty. Journal of Mechanical Design **134**(3), 031,008 12 pages (2012)
26. Sanson, F., Maitre, O.L., Congedo, P.M.: Systems of gaussian process models for directed chains of solvers. Computer Methods in Applied Mechanics and Engineering **352**, 32 – 55 (2019). DOI https://doi.org/10.1016/j.cma.2019.04.013. URL http://www.sciencedirect.com/science/article/pii/S0045782519302105
27. Sasena, M.K.: Flexibility and efficienvy enhancements for constrained global design optimization with Kriging approximation. Ph.D. thesis, University of Michigan (2002)
28. Sellar, R.S., Batill, S.M., Renaud, J.E.: Response surface based, concurrent subspace optimization for multidisciplinary system design. In: 34th AIAA Aerospace Sciences Meeting and Exhibit, pp. 96–0714 (1996)
29. Shi, R., Liu, L., Long, T., Wu, Y., Wang, G.G.: Multidisciplinary modeling and surrogate assisted optimization for satellite constellation systems. Structural and Multidisciplinary Optimization **58**(5), 2173–2188 (2018). DOI 10.1007/s00158-018-2032-1. URL https://doi.org/10.1007/s00158-018-2032-1
30. Sobieszczanski-Sobieski, J., Haftka, R.T.: Multidisciplinary aerospace design optimization: survey of recent developments. Structural optimization **14**(1), 1–23 (1997)
31. Wang, X., Li, M., Liu, Y., Sun, W., Song, X., Zhang, J.: Surrogate based multidisciplinary design optimization of lithium-ion battery thermal management system in electric vehicles. Structural and Multidisciplinary Optimization **56**(6), 1555–1570 (2017). DOI 10.1007/s00158-017-1733-1. URL https://doi.org/10.1007/s00158-017-1733-1
32. Xu, C.Z., Han, Z.H., Zhang, k.s., Song, W.: Surrogate-based optimization method applied to multidisciplinary design optimization architectures. In: 31st Congress of the International Council of the Aeronautical Sciences (ICAS 2018) (2018)
33. Zhang, M., Gou, W., Li, L., Yang, F., Yue, Z.: Multidisciplinary design and multi-objective optimization on guide fins of twin-web disk using kriging surrogate model. Structural and Multidisciplinary Optimization **55**(1), 361–373 (2017)

7 Appendix

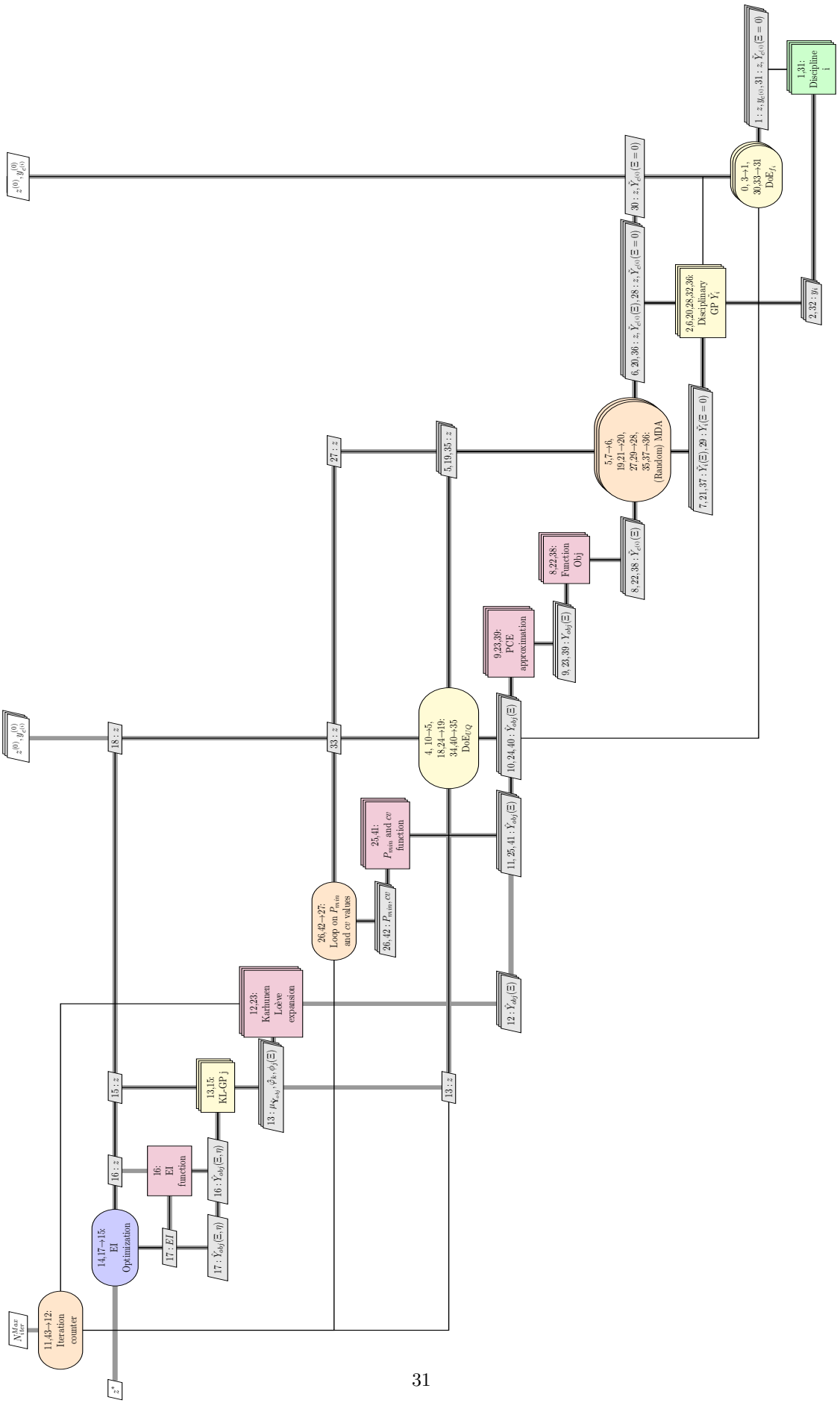

Fig. 26 XDSM (eXtended Design Structure Matrix [17]) of the EGMDO process.